



Università
Ca' Foscari
Venezia

Master's Degree programme – Second
Cycle (*D.M. 270/2004*)

Department of Environmental Sciences

Master's Degree Programme in Environmental Sciences

Final Thesis

*Determination of Trace elements and Major Ions in
Environmental Matrices from Rano Raraku Lake (Easter Island)*

Supervisor

Dr. Dario Battistel

Graduand

Shahpara Hanif

Matriculation Number: 865270

Academic Year

2017/2018

Page intentionally left blank

ABSTRACT

Easter Island is located in the southern Pacific Ocean and it is famous for its megalithic statues named 'moai'. Two lakes Rano Raraku (RR) and Rano Aroi (RA) are central water resources currently used by the local population for agricultural and breeding activities. The objective of this study is to determine the trace and rare earth elements as well as major ion contents in their water and in soil collected in the lake basin to obtain information about the water quality and to provide additional insights on transport mechanism inside the lake basin. The analysis was carried out by using Inductively Coupled Plasma – Mass Spectrometry, Isotope Ratio Mass Spectrometry and Ion Chromatography.

The results showed that RR water contains high amounts of sodium and chlorine due to high evaporation rate in conjunction with a likely marine input. These values make the water undrinkable and unsuitable for agricultural purposes, although the level of metals in the water is not alarming. The rare earth element analysis suggested that strong winds activity, favored by the high deforestation rate occurred several centuries ago, is the main factor that influenced transport dynamics inside the basin. Potential warning for the water quality of RR is due to the unregulated management of the wild horses, as the dead body of the animals that often times left near lakeshore. RR and RA are found to enrich in Ag, Fe, and Zn but they are deficient in many elements like Cs, Pb, V, and Ni. This is explained as Island does not have industrial activities. Although the water of Rano Aroi is not polluted by metals and the presence of dead animals was not observed, the recent plantation of the eucalyptus forest in its neighborhood is a serious thread that may cause significant drop in the level of water in the next future.

Keywords: Easter Island, Rano Raraku, Rano Aroi, rare earth and trace elements, major ions, enrichment and deficient factors

ACKNOWLEDGEMENTS

Without acknowledging the contribution of dynamic and talented individuals; I cannot move further. Infact; it was quite impossible to conduct this research study without the support of my supervisor and colleagues working in Institute for the Dynamics of Environmental Processes, National Research Council of Italy (IDPA-CNR).

I am especially thankful to Dr. Dario Battistel, Research Scientist from Department of Environmental Science, Informatics and Statistics (DAIS), Ca' Foscari University of Venice; who has been supportive throughout the research period including sampling, experimentation and drafting. I really appreciate for his academic time received to pursue the objectives of this research.

Additionally, I would like to thank Dr. Clara Turetta (From IDPA-CNR) for a continuous support in instrumentation for this research. This helped me to efficiently derive necessary results for further optimization.

Last but not the least; a special thanks to my loving husband; Dr. Saif Maqbool (Assistant Professor, National University of Computer & Emerging Sciences, Pakistan) for an unconditional & enormous support that kept me on learning track throughout the master studies.

Thank you very much!

TABLE OF CONTENTS

Contents

ABSTRACT.....	3
ACKNOWLEDGEMENTS.....	4
TABLE OF CONTENTS.....	5
LIST OF TABLES.....	8
LIST OF FIGURES.....	10
1. INTRODUCTION.....	12
1.1 Easter Island: the study site.....	14
1.2 Archaeological Context.....	21
1.3 Topographic Characteristic.....	23
1.3.1 Rano Raraku.....	24
1.3.2 Rano Aroi.....	26
1.4 Vitiation of lake water.....	27
2. MATERIALS & METHODS.....	30
2.1 Samples.....	30
2.1.1 Rano Raraku water samples.....	30
2.1.2 Rano Raraku soil samples.....	33
2.2 Rano Aroi water sample.....	34

3. INSTRUMENTATION	34
3.1 Coupled Plasma – Mass Spectrometry (ICP-MS)	35
3.1.1 ICP-Quadrupole MS (ICP-MSQ)	36
3.2 Ion Chromatography	37
3.3 High Temperature Conversion Elemental Analyzer Isotope ratio mass spectrometry (HTC-RIMS).....	39
4. METHODOLOGY	41
4.1 Analysis of trace and rare earth elements in water samples	41
4.2 Analysis of soil and filter samples:.....	41
4.3 Analysis of Cations and Anions in water samples.....	42
4.4 Isotopic analysis of $\delta^{18}\text{O}$ and ^2H in water sample.....	43
4.5 Statistical analysis of the data.....	44
4.5.1 Equations used to calculate fractionation dynamics, ratio of LREE/HREE and Cerium anomaly.....	44
4.5.2 Calculation of enrichment factor and depletion factor	46
5. RESULTS	48
5.1 Concentration of trace elements in Rano Raraku and Rano Aroi.....	48
5.2 Concentration of rare earth elements in Rano Raraku and Rano Aroi	52
5.3 Ions analysis of water samples of Rano Raraku and Rano Aroi.....	54
5.4 Isotopic Analysis.....	54

5.5.1 Enrichment factors	55
5.5.2 Depletion factor	58
5.6 Low Rare Earth Elements / High Rare Earth elements ratio (LREE/HREE)	61
5.7 Cerium Anomaly	64
6. Discussion	68
CONCLUSION	71
References	72

LIST OF TABLES

Table 1: Details of collected water samples from Rano Raraku.....	31
Table 2: Details of Rano Raraku sites selected for collection of soil samples along with coordinates and date of collection.....	34
Table 3: Details of water and filtered sample collected from Rano Aroi	34
Table 4: Trace element concentration in soil and water samples of Rano Raraku and Rano Aroi	50
Table 5: Rare earth element concentration in soil and water samples of Rano Raraku and Rano Aroi.....	53
Table 6: Presence of cations and anions in water samples of Rano Raraku and Rano Aroi	54
Table 7: Isotopic enrichment of $\delta^{18}\text{O}$, δD and d-excess values of water samples.....	55
Table 8: Enrichment Factor values of Rare earth elements and trace elements found in Rano Raraku.....	57
Table 9: Depletion factor of rare earth elements and trace elements in Rano Raraku.....	60
Table 10: Normalized values of rare earth elements with NASC in Rano Raraku.....	61
Table 11: Presence of possible outliers in the distribution in the matrices of LREE/HREE in soil, water, filtrate and Σ (Filt+Water).....	62
Table 12: Final values of variance, Std. dev. (S) and degree freedom of groups for Rano Raraku	62

Table 13: Shapiro-Wilk test of four groups	63
Table 14: Comparison between four groups and their F_{calc} , F_{crit} , p-value and Homogeneity.....	63
Table 15: Comparison of four groups values.....	64
Table 16: Values obtained for cerium anomaly in water, soil, filtered and water + soil samples.....	65
Table 17: Results obtained in Dixon test and presence of possible outliers in the distribution matrices.....	66
Table 18: values of variance and mean in four groups water , soil, filtered and water + soil samples.....	66
Table 19: Shapiro-Wilk test for four groups.....	67

LIST OF FIGURES

Figure 1: Location Map	15
Figure 2: Main Sources of rainfall in Easter Island (Núria Cañellas-Boltà et,al 2016)....	16
Figure 3: Precipitation map of Ester Island, colours from dark brown to dark blue shows increase in amount if precipitation (Cedric O. Puleston at,al 2017).....	17
Figure 4: Vegetation	19
Figure 5: Planted Eucalyptus forest	20
Figure 6: Moais on Easter Island	21
Figure 7: Rano Raraku Crater Lake	25
Figure 8: A) Rano Aroi lake B) Forest of Eucalyptus C) Intermittent herbaceous marshes and swamps.....	27
Figure 9: Agricultural Activities.....	28
Figure 10: shows horses are drinking water from near to sea shore	29
Figure 11: Collection of water sample from RR.....	32
Figure 12: Shows schematic diagram of a typical ICP-MS setup	36
Figure 13: Quadrupole Mass Analyzer system of an ICP-MS	37
Figure 14: Picture of a typical instrument of Ion Chromatography.....	39
Figure 15: Systematic Diagram of HTC-RIMS Isotopic Analysis ofO and H Isotopes ...	40
Figure 16: Soil and filter paper samples treated with HNO ₃ and HF	42

Figure 17: Diluted water samples of different concentration	43
Figure 18: Enrichment Factor values of Rare earth elements and trace elements found in Rano Raraku.....	56
Figure 19: Trend of “Depletion factor” of rare earth elements and trace elements in Rano Raraku	59

1. INTRODUCTION

Water is a vital natural resource and its availability affects social, economic, ecological and sustainability. For all living organisms and ecosystems water quality is as important as water quantity. Many ecosystems processes are derived directly from water and agricultural activities mainly in semi-arid and arid climate zones depending on the availability of fresh water (UNESCO 2012). Climate change causes crucial threats to global water supply such as vulnerability and degradation of freshwater reservoirs.

Worldwide extraction rate of fresh water for agricultural purposes has tripled over the past 50 years. Moreover, the abstractions of water in many basins have exceeded the recharge rate. Thus, as a consequence, fresh water source cannot be considered sustainable (UNESCO 2012). As water reservoirs are over-exploited, considerable losses of habitat and biodiversity were observed, as well as impacts on the ecological integrity of streams and wetlands (Ribeiro and da Cunha, 2010).

Among freshwater sources, lakes are an indispensable source of freshwater for human settlements. Surface waters in large, shallow lakes are characterized by high degree of spatial and temporal heterogeneity (Riffat Naseem Malik and Muhammad Nadeem, 2011). Physical and chemical characteristics of surface water of lakes are generally largely determined by the climatic, geochemical and geomorphologic conditions. The variation in quality of water also depends on surrounding vegetation, and land-use activities in the catchment basin (Hanh et al. 2010). However, characteristics of lake water and the ecological integrity of aquatic ecosystems is highly influenced by natural processes like precipitation rate, weathering processes, soil erosion and human-related activities (Qadir et al. 2008).

Freshwater can be contaminated by anthropogenic activity, generally through air- or waterborne contamination. These pollutants can enter from point sources that are known pathway of contaminants, or diffuse sources where the contaminants enters the lake with unknown specific point of discharge (European Environment Agency, 2008). A lake can be used for the disposal of municipal solid, agricultural and industrial waste. After disposal of waste in lakes, the waste undergoes chemical, physical and biological changes (Kjeldsen et al., 2002). Part of the pollutants entering in the lake may dissolve into the water, while the heavier particles will settle into the sediment at the bottom. Rainfall water entering a lake can result in leaching of compounds into the infiltrating water. The resulted polluted water is called leachate. This leachate may contain many different substances, for example organic matters, organic and inorganic pollutants as well as metals.

Metals are natural constituents of the earth crust; they can be present either at high or very low concentrations as trace elements (TE). Soil and sediments constitute reservoirs of TE as they are non-biodegradable hence they persist and accumulate in the soil (Gleyzes et al., 2002). Beside them, rare earth elements (REE) also constitute the earth crust, across the lanthanide series from La to Lu. The systematic decrease in ionic radius as a function of the atomic number provides a predictable chemical variation which can help to record precisely geochemical processes in natural systems. Groundwaters can obtain unique REE signatures that are characteristic of the rocks through which they interact with (e.g. Smedley 1991; Johannesson et al. 1997 and 2000). Therefore, the REE amount and several diagnostic ratios can be used to study weathering processes in rocks and soil as well as the evolution of groundwater (Nelson et al., 2004).

1.1 Easter Island: the study site

Easter Island is a volcanic island situated in the southern Pacific Ocean $27^{\circ}09'30''\text{S}$ latitude and $109^{\circ}24'14''\text{W}$ longitude. Maunga Terevaka, Kao and Poike are three volcanic cones fused together, and merged to form a roughly triangular Island of nearly 164 km^2 . Beside these three volcanoes, this island has around 70 other minor satellite cones (Rull et al. 2015). The highest point is the summit of the Terevaka volcano (511 m). It is one of the most geographically isolated places in the world as it is placed 3,700 km away from the Chilean coast. Figure 1 shows the map of Easter Island and the location of the summit of Terevaka volcano. The island has an essential archeological value, especially due to the large stone sculptures known as “Moais” and their mysterious disappearance of its ancient civilization that is still not completely explained by the archeologists.

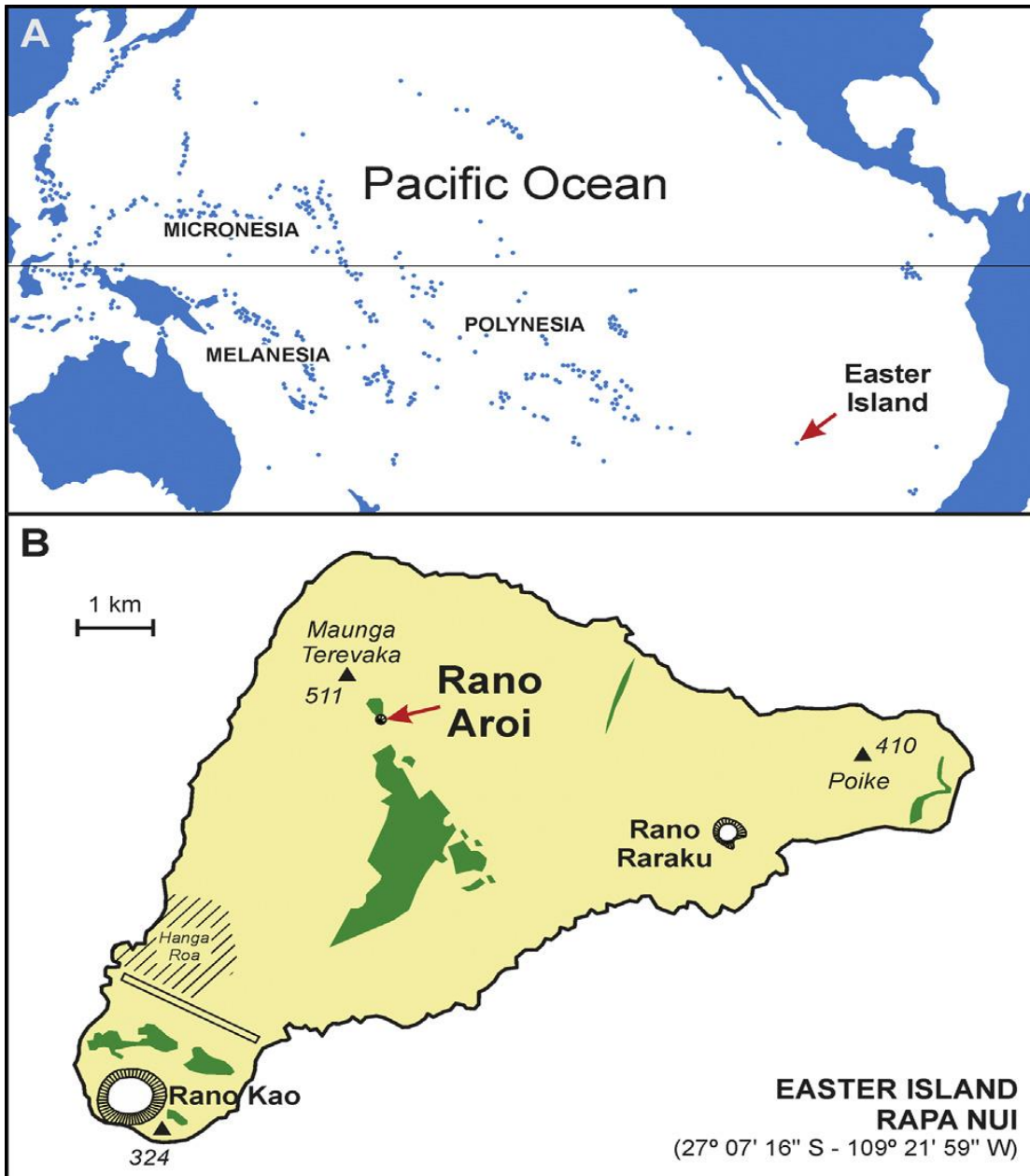


Figure 1:Location Map

A) Easter Island in the Pacific ocean

B) Sketch-map of the island showing the study site Rano Aroi and Rano Raraku - Green areas indicate the Eucalyptus forests planted recently (Rull et,al 2015).

Easter Island climate is subtropical, with average monthly temperatures that range between 16 (July-September) and 26°C (January-March). The total amount of annual precipitations is highly variable ranging from 500 to 2000 mm. From April to June, maximum

rainfalls occur while October is driest month about 70 mm rainfall occurs in this month (Azizi and Flenley, 2008). Main rainfall sources are the South Pacific Anticyclone, the South Pacific Convergence Zone, the Intertropical Convergence Zone and the Westerly storm tracks (Margalef et al. 2013; Sáez et al. 2009). Figure 2 shows a map of these atmospheric systems.

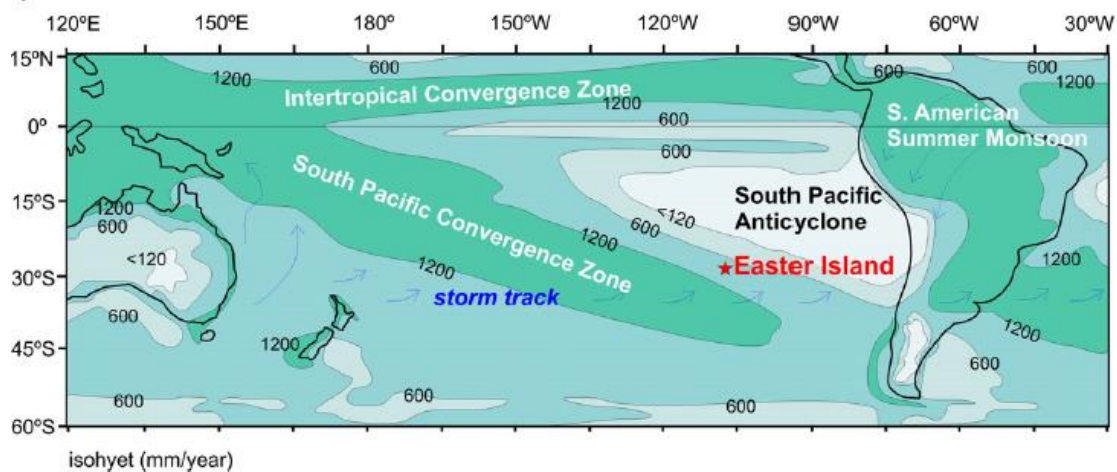


Figure 2: Main Sources of rainfall in Easter Island (Núria Cañellas-Boltà et,al 2016)

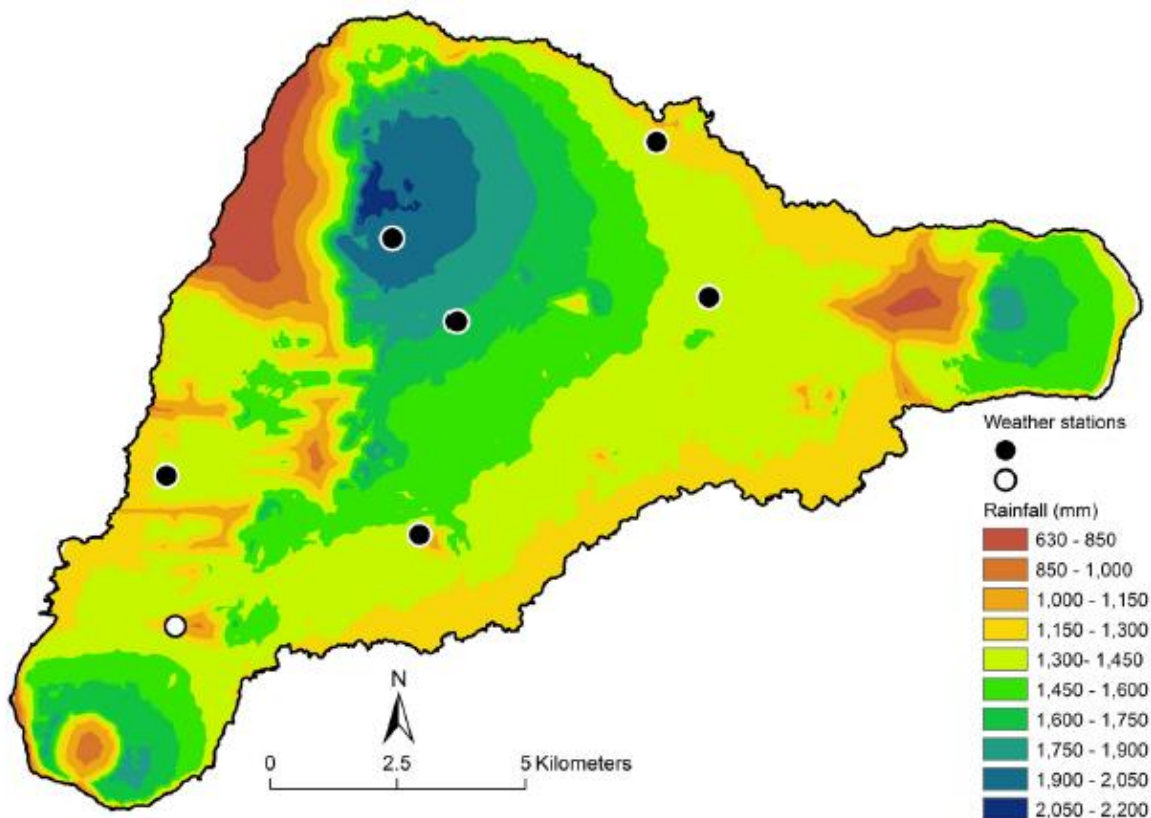


Figure 3: Precipitation map of Ester Island, colours from dark brown to dark blue shows increase in amount of precipitation (Cedric O. Puleston et al., 2017)

Figure 3 shows the annual amount of rainfall received by Island; six black dots indicate weather stations. In the southwest white dot shows the rain shadow area; it is located on elevation of 69 m asl and expected rainfall is 1,361mm but actual annual rainfall received is 1,097 mm. The driest parts of the Island are west of Poike and extreme east of the island peninsula.

Prominent feature of Ester Island is its low biological diversity, probably because of its isolation and small size. Island has flora of only 46 species including the both extinct *Jubaea* palm and the *toromiro* tree that were endemic in the past (Dransfield et al., 1984). Similarly, the fauna in the island is also depauperate in the terrestrial vertebrates and invertebrates. The fauna

does not have endemics (Campos and Pena, 1973). However, many exotic species have been introduced by humans.

Many evidences suggest that the island was covered by dense forests until the 17th century. From macrofossils analysis thirteen species of trees and shrubs have been found. Most of them have living relatives in few other Pacific islands, such as Tahiti and Rarotonga (Orliac, 2000). Palynological evidences suggested that formerly toromiro (*Sophora toromiro*), *Compositae* and palm trees (*Pritchardia*) were abundant in the island until few centuries ago (Flenley and Bahn, 2002).

Currently, about the 90% of the Island is covered by grasslands dominated by *Sporobolus indicus* and *Paspalum scrobiculatum*. Shrubland occupies nearly the 4% area that is dominated by the invader *Psidium guajava* (Myrtaceae). Urban and pioneer vegetation covers nearly the 1% of the area. Among them, prominent species are *Psidium guajava*, *Crotalaria sp.* and *Lupinus arboreus* (CONAF 1997). Figure 4 shows the land occupied by aquatic vegetation, grasses and shrubs.

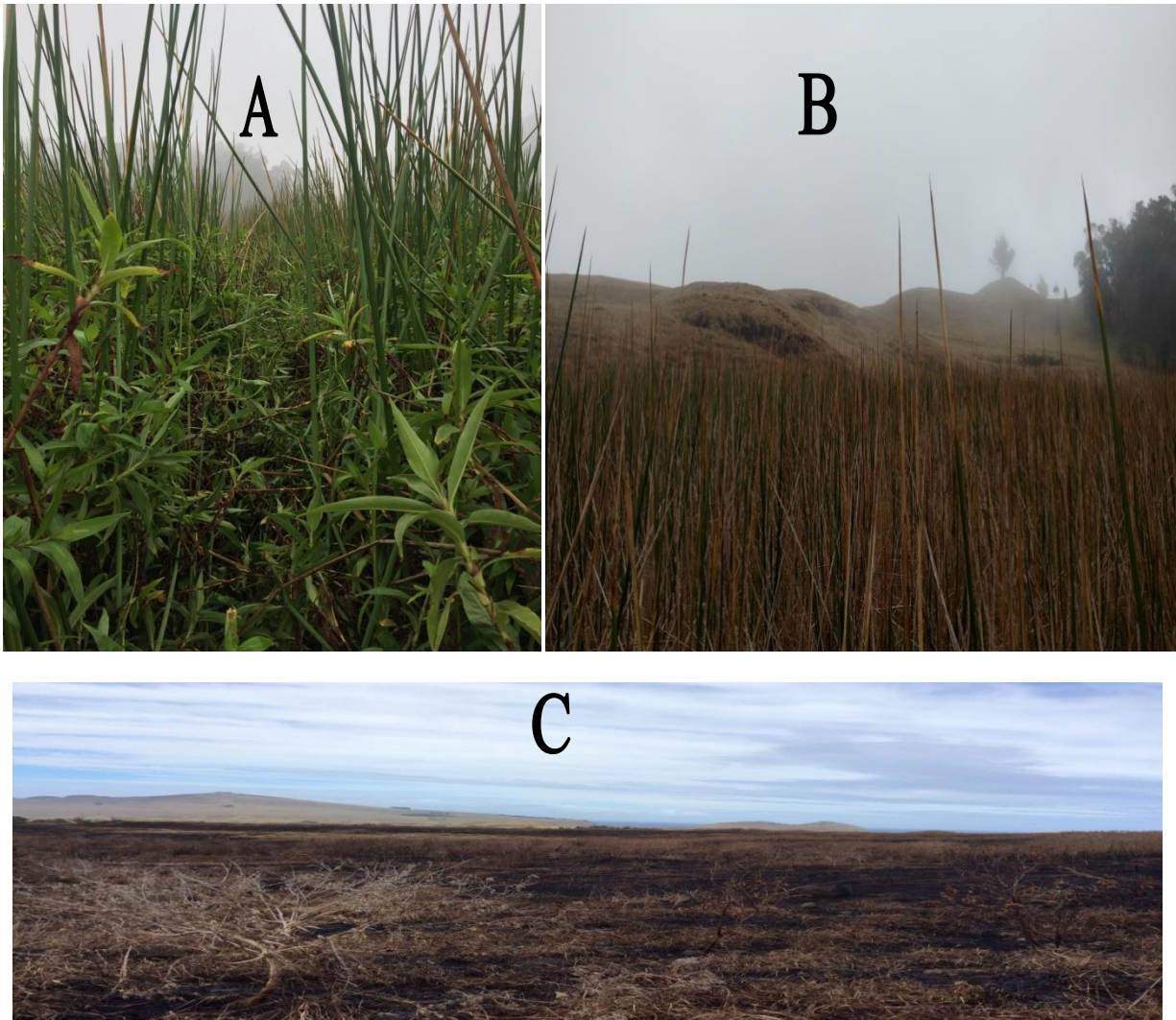


Figure 4:

- A) Aquatic vegetation, *Scirpus californicus* (Cyperaceae) & *Polygonum acuminatum* (Polygonaceae)
- B) Grasses, *Sporobolus indicus* and *Paspalum scrobiculatum*,
- C) Shrubs dominated by the invader *Psidium guajava*

The angiosperm flora of the island has 179 species, of which 141 are introduced, 30 are autochthonous and 8 are of uncertain origin. In the autochthonous flora, species of family Asteraceae and Fabaceae are very common (Zizka, 1991). *Axonopus paschalis* (Poaceae), *Sophora toromiro* (Fabaceae), *Danthonia paschalis* (Poaceae) and probably *Paspalum forsterianum* (Poaceae) are endemic in Easter Island. Human activities, livestock (notably

horses) and the introduction of aggressive invader species are serious threat to the flora and the vegetation of Easter Island. In particular, the inner slopes of Rano Kao could serve as site for the conservation of the local flora (Zizka, 1993).

Today, eucalyptus forests covers about the 5% of the island. Indeed, during the 1900, the reforestation is carried out by planting Eucalyptus trees because of its fast growing characteristic. Another round of planting was followed in the 1960-1970s. As it shown in Figure 1, plantation of Eucalyptus forest corresponds with the green color areas. The more common *Eucalyptus spp.* are Myrtaceae and *Dodonaea viscosa* (Sapindaceae) (V. Rull et al. 2010). Figure 5 shows the planted forest of Eucalyptus. The reforestation is extremely important for the island protection against further soil erosion.



Figure 5: Planted Eucalyptus forest

Source: <https://www.dw.com/en/bringing-the-trees-back-to-easter-island/a-18366801>

1.2 Archaeological Context

The Rapa Nui society that erected the moai vanished from the ancient Eastern Island culture is considered a dramatic cultural shift of the Island. The society that carved these moais is called the Ancient Cult or the moai cult. They used soft volcanic rocks of Rano Raraku crater for carving the raw material for creating the moai. Thus, the moai cult society was settled around crater of Rano Raraku. Figure6 shows the picture of some moais. Then, the unknown significant changes happened in their lifestyle, sociopolitical organization, religious performance, art and also in the geographical settlement of the culture that this society was replaced by the Birdman-Cult society, based on Rano Kao, to the western part of the island. Many theories suggested such geographical change and societal transformation.



Figure 6: Moais on Easter Island

Generally, the Ester Island history can be divided into three phases: early (from 5th century colonization to c. 1100 AD), middle (c. 1100 to c. 1680 AD), and late (c. 1680 AD to the present). The last era is characterized by decadence and collapse, as consequences of the overpopulation and overexploitation of resources (Henri J. Dumont et.al 1998).

Although, still it is not unanimous decision of archeologists when humans first discovered Rapa Nui (Hunt and Lipo, 2006) but it is clearly marked that from ca. AD 1200 primeval forest were destroyed. The most well-known theory that explains the disappearance of the ancient culture that built the iconic megalithic statues is the ecocidal hypothesis. According to this cultural collapse, it happened because of the exhaustion of natural resources as a result of human overexploitation (Bahn and Flenley, 1992; Flenley and Bahn, 2003; Diamond, 2005). According to this theory, Rapa Nui (habitants of Easter Island) did reckless cutting of forests for agricultural purposes and construction of huge sculptures Moais.

Around AD 1650 human population rose to uncontrolled level. Many archeologists claimed that trees were cut down by the ancestors of today's Easter Islanders so, they could transport the giant stone statues Moai and build houses, canoes and fires to burn their dead. Hence, due to the massive deforestation, the Rapa Nui soon ran out of their natural resources, they had no more firewood and materials to make canoes to go fishing in the sea. Therefore, the areas closest to the coast were quickly overfished and the island's birds wiped out. Massive scale deforestation caused surface soil exposure to the heavy rain and strong trade winds so, the upper layer of soil eroded away and turned unsuitable for agricultural purposes. As a result of such harsh conditions, wars broke out over competition of few available resources. It is also believed that the islanders resorted to cannibalism to survive, hence Easter Island society collapsed (Michael Marek, DW article 2015). This interpretation of Easter Island history makes the basis for developing general models for human use of natural resources (Brander and Taylor, 1998; Dalton and Coats, 2000; Reuveny and Decker, 2000).

Many cases of societal collapse occurred on basis of external environmental changes, thus, another interpretation gives that environmental changes, beyond the control of humans,

triggered the societal collapse of Rapa Nui (Nunn, P. D. 2000; Orliac, C. 2005; Diamond (2005). However, the main limitation in this interpretation as the Ester Island is geographically isolated so, it is difficult to infer its environmental history from better known regions. Therefore, its paleoenvironmental history is not well understood to test hypotheses involving climate change as causes of societal collapse (Daniel Mann et al. 2007).

Another hypothesis gives that eventual collapse of this society was independent from the ecological catastrophe and several authors proposed a “genocidal” hypothesis (Daniel Mann et al. 2007). European explorers introduced disease organisms into an immunologically native population. As initial deforestation was also a collaborative impact of Polynesian settlers and their commensal rat: *Rattus exulans*. It is suggested that, as rats have high reproductive rate, during an irruptive, rat-outbreak interval, they strongly damaged the native plants and animals. Due to lack of empirical support this hypothesis was also rejected (V. Rull et al., 2015)

Although any archaeological interpretation is out of the scope of this thesis, it is important to underline that the management of water resources is not only a present-days issues as it may have contributed to influence even the past Rapa Nui societies.

1.3 Topographic Characteristic

Main topographic characteristic of Ester Island is its volcanic cones and the rolling surfaces of the lava that have flown between them. Due to the high permeability of the volcanic rocks, no permanent surface streams are present (Herrera and Custodio, 2008). At present time, only three major permanent fresh water bodies are present, the craters of Rano Raraku and Rano Kau (occupied by lakes), and Rano Aroi (filled by a swamp) along with numerous small springs and stagnant pools (Cañellas-Boltà et al., 2012). Rano Raraku and Rano Kau are two major

archaeological sites, that are the statue Quarries and the Orongo village, respectively. As this thesis is focused on the two main crater of Rano Raraku and Rano Aroi I will provide a more detailed description in the following paragraphs.

1.3.1 Rano Raraku

Rano Raraku is formed more than 300,000 years ago. It occupies small area of 0.11 km² situated at 75 m altitude inside a volcanic crater. The lake only source of water is precipitation, as impermeable lacustrine sediments disconnected it from the island's main groundwater (Herrera and Custodio, 2008). Its catchment area is about 0.35 km², mainly constitute of volcanic tuff rich in glass, feldspar, iron oxide, clay minerals and pyrite aggregates. The lake water is acidic by pH around 6.3 and diluted average specific conductivity is 640 $\mu\text{S cm}^{-1}$ (Cañellas-Boltà at al. 2012). Today surface of lake has large floating patches formed by the mat of *Scirpus californicus*. The excess amount of pumping out water for domestic uses and less amount of the rainfall occur as compare to the past due to global environmental changes has significantly lowered the water level during the last decades. Figure 7-A and 7-B shows the fast changes in the lake level at Rano Raraku during the period between September 2017 and March 2018.

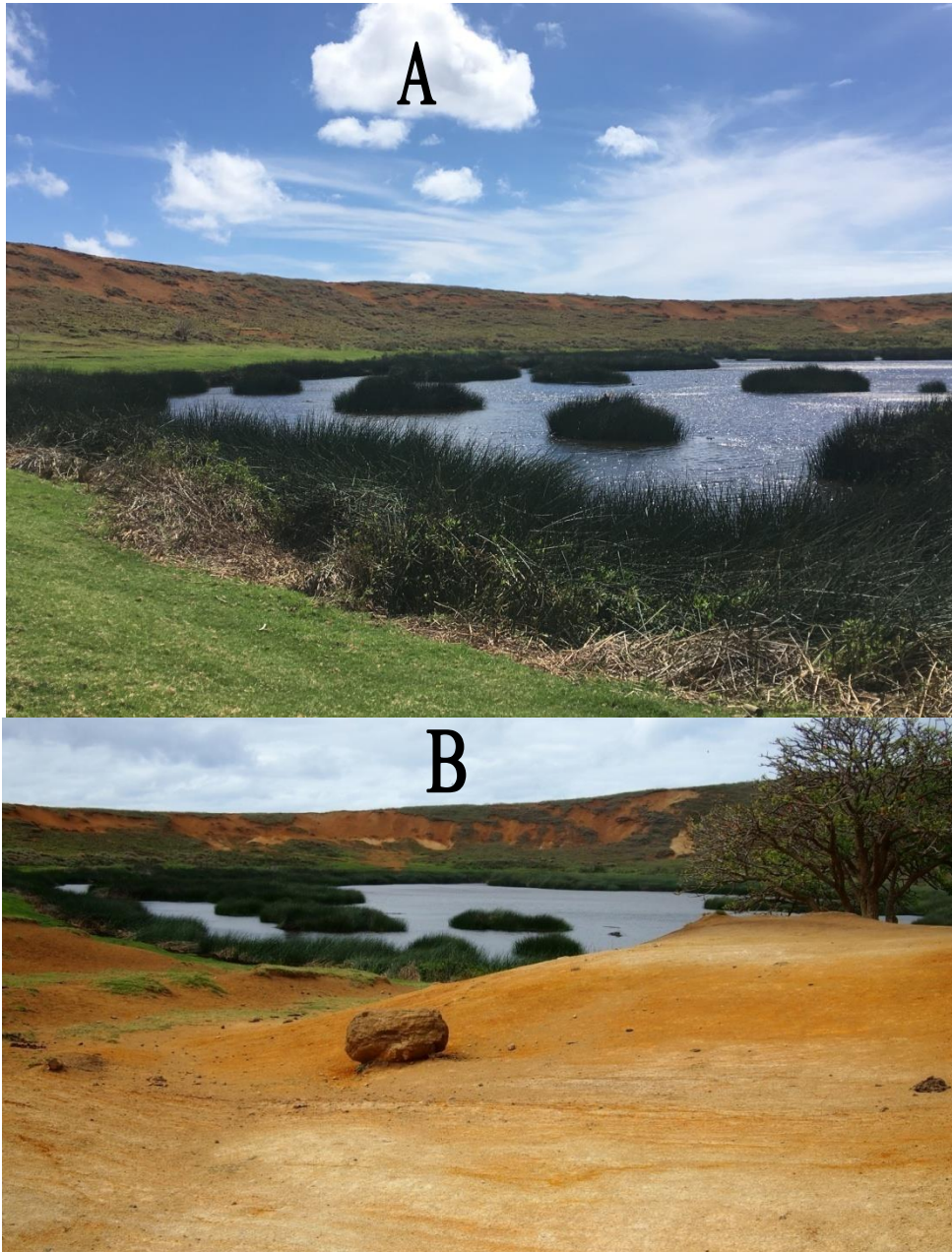


Figure 7:
A - Rano Raraku crater lake
B - Decrease in water level.

The asymmetric and the complex geological origin of the Rano Raraku crater is famous for the source of the *moai* sculptures (Baker & Buckley, 1974). Its south and southeast rims inner and outer walls were cut to carve *moai*. While quarrying statues large amount of erosive material and unfinished statues washed into the lake and added into debris of lake sediment layer. Most

assumptions about Easter Island's palaeoecology and palaeoclimatology are derived from the Rano Raraku lake sediments (Butler and Flenley, 2010; Horrocks et al., 2102).

In every year new layer of sediments is formed on the top of what has already accumulated. As each year microscopic algae grow and after completion of its biological season died and accumulate to the bottom of the lake along with any clay or silt washed into the lake from the slopes surroundings. Many particles such as pollen grains brought by air also fall into the layer of sediments. Thus they all constitute to make new sediment layer. This process is carried out since the lakes formed over thousands of year ago. In recent century this process has accelerated because of the totora reed (*Scirpus riparius*) and sub-aquatic plant, tavai (*Polygonum acuminatum*). They grow in edges of lakes and during dry seasons extend their growth right over the sediment surface and cause rapid growth of new sediments (John Felenly and Paul Bahn the Enigmas of Easter Island). These sediments have great potential to provide information about palaeo-environment of the island, and human impact on it.

1.3.2 Rano Aroi

Rano Aroi crater is located in an ancient Pleistocene volcano crater that is near to highest summit of the island. It outflows through a small creek that infiltrates downstream for about 400 m. This lake has is a mire of ~150 m diameter and situated at 430 m elevation. The lake is formed by rainfall and groundwater and serves as a minerotrophic fen. As it is near to the top, it can easily subjected to seasonal variations and even desiccation (O. Margalef at al. 2014). Water level is significantly dropped due to construction of an artificial outlet in the 1960s and seasonal variations in precipitations (Herrera and Custodio, 2008).

Rano Aroi is covered by andosols and constitute of porfiric, olivinic, tholeiite, hawaiiite, and basaltic lava. Surrounding area is covered by intermittent herbaceous marshes and swamps dominated by Cyperaceae, grasses and a small eucalyptus forest. Surface vegetation is marked by *Polygonum acuminatum*, *Asplenium polydon* var. *squamulosum*, *Scirpus californicus*, *Cyclosorus interruptus* and *Vittaria elongate* (V. Rull et al., 2010). Figure 8 shows the RA with Eucalyptus forest, herbaceous marshes and swamps. Hydrogeological studies confirm that Rano Aroi water system represents perched spring connected to the main island aquifer (Herrera and Custodio, 2008).



Figure 8: A) Rano Aroi lake B) Forest of Eucalyptus C) Intermittent herbaceous marshes and swamps.

1.4 Vitiation of lake water

At present, people of Ester Island carried out cultivation of some crops like different vegetables for domestic use. In Figure 9a cultivation of tomatoes and taro root is displayed. In the island, an efficient irrigation system is not present mainly they rely on water of these three lakes, rainfall or mostly from external supply. Due to the not proper check and management of

domestic animals, especially horses, the water quality of the lakes is significantly damaged: Indeed, wild animals directly contaminate water from their waste material (feces and urine). Moreover, when they die, instead of their proper disposal, they are left in open environment later along with rainfall water they flow in the lake. Hence, they become cause of water contamination of the lakes. Figure 9b shows a dead horse in proximity of Rano Raraku. These unregulated practices may potentially cause eventual diffusion of infection among other animals.



Figure 9:

a. Agricultural activity for domestic purpose.

b. Dead horse at the edge of lake

On visit to Island people of Rapa Nui claimed that almost two centuries before ancient people used to drink water from the sea (Battistel, personal communication). Their claim can be true. In Figure 10 it can be seen horses are drinking water from very near to sea shore, in actual process this is the point where ground water enters into the sea, as density of ground water is lower than sea water. Thus the upper layer of water is composed of fresh water while lower layer is of sea water.

The uniqueness in culture and the exotism of the island made it a national and international tourist attraction since the 1990s. Hence, number of visitors has largely increased; consequently there is increase demand of fresh water. Due to unsustainable use and exploitation of water of these lakes are drying up. Moreover, high rate of evaporation due to strong winds and

drastic change in weather conditions causes less rainfall are also contributing to considerable fall in water level of lakes.

Rano Raraku and Rano Aroi are potentially influenced by multiple points, nonpoint mining and agricultural sources of contaminants. A comprehensive assessment of water and sediments samples from these lakes provides the information about the chemical composition of lake water quality. Presence of trace elements, rare earth elements ions and organic contents, help to draw conclusion about quality of lake water.



Figure 10: shows horses are drinking water from near to sea shore

2. MATERIALS & METHODS

The overall analyses were carried out at the Analytical Chemistry laboratories at Ca' Foscari University of Venice and at the national research council institute of dynamics environmental processes (CNR-IDPA) located at the campus Scientifico via Torino, Mestre-Venezia, Italy.

2.1 Samples

All the samples were collected at Ester Island in two distinct sites corresponding to the lakes named Rano Raraku (27.1239° S, 109.2861° W) and Rano Aroi (27.0844° S, 109.3794° W) located as shown in Fig 1B. Six water and soil samples were collected from Rano Raraku, while only a single sample of water was collected from Rano Aroi, due to the formal restrictions imposed by the local authorities.

2.1.1 Rano Raraku water samples

A total amount of 6 water samples were collected using a 0.5 l PE bottle from Rano Raraku on 7th September 2017 in three different locations (named P1, P2 and P3 : GPS coordinates are reported in Table 1). Figure 11a, shows collection of water sample from RR. At each location, a surface (S) and a corresponding bottom water sample at a depth of 90, 51 and 38 cm, for P1, P2 and P3, respectively, were collected. All the samples were filtered in situ, as shown in Figure 11b, through a 0.45 μ m cellulose filter paper (Whatman) using a polycarbonate filtering system equipped with a manual vacuum pump. Different amounts of water, ranging from 250 to 475 mL, were filtered, depending on the amount of particulate matter contained, that limit the drainage ability of the pump. Filter (F) and water (W) samples were stored in refrigerator before analysis. All details about filter and water samples are summarized in Table 1.

Each sample was labeled as RR-X-Y-Z where X refers to the matrix (water or filter), Y refers to the location and Z refers to the depth.

Table 1: Details of collected water samples from Rano Raraku

Lake		Date - Collection	Date - Filtered	Position	Latitude	Longitude	Depth (cm)	Sample	#Name
Rano Raraku	RR	7/9/2017	7/9/2017	P1	-27.1222	-109.29	S	F	RR_F_P1_S
Rano Raraku	RR	7/9/2017	7/9/2017	P2	-27.1221	-109.29	S	F	RR_F_P2_S
Rano Raraku	RR	7/9/2017	7/9/2017	P3	-27.1222	-109.29	S	F	RR_F_P3_S
Rano Raraku	RR	7/9/2017	7/9/2017	P1	-27.1222	-109.29	90	F	RR_F_P1_90
Rano Raraku	RR	7/9/2017	7/9/2017	P2	-27.1221	-109.29	51	F	RR_F_P2_51
Rano Raraku	RR	7/9/2017	8/9/2017	P3	-27.1222	-109.29	38	F	RR_F_P3_38



**Figure 11: a) Collection of water sample from RR
b) In field filtration of water samples by polycarbonate filtering system**



Figure 11:c)Shows selected site for collection of soil sample

2.1.2 Rano Raraku soil samples

Six soil samples were collected in four different sites named P4, P5, P6 and P7 on 7th September at Rano Raraku. In P5 and P6 two soil samples were collected for each location. Coordinates and other details are shown in Table 2. Figure 11c shows picture of selected site. These samples were brought to the laboratories and they were thawed and dried in an oven at 105°C for 24 hours before analysis. The dried sediment samples were grinded and stored in a desiccator before the analysis.

Table 2: Details of Rano Raraku sites selected for collection of soil samples along with coordinates and date of collection

Lake	Date - Collection	Position	Latitude	Longitude	Depth (cm)	Sample	#name
Rano Raraku	RR 9/9/2017	P4	-27.1222	-109.29067		S	RR_S_P4_
Rano Raraku	RR 9/9/2017	P5	-27.1216	-109.2906	A	S	RR_S_P5_A
Rano Raraku	RR 9/9/2017	P5	-27.1216	-109.2906	B	S	RR_S_P5_B
Rano Raraku	RR 9/9/2017	P6	-27.1205	-109.28828	A	S	RR_S_P6_A
Rano Raraku	RR 9/9/2017	P6	-27.1205	-109.28828	B	S	RR_S_P6_B
Rano Raraku	RR 9/9/2017	P7	-27.1246	-109.28939		S	RR_S_P7_

2.2 Rano Aroi water sample

One single water sample was collected from Rano Aroi, corresponding to the following coordinates: -27.094679; -109.373912 on 9th September 2017. This single sample is then labeled as RA-W-PO-S. The sample RA-W-PO-S was collected from surface of lake and 100mL of sampled water was filtered on 12th September 2017. Further details are reported in Table 3.

Table 3: Details of water and filtered sample collected from Rano Aroi

Lake	Date - Collection	Date - Filtered	Position	Latitude	Longitude	Depth (cm)	Sample	#name
Rano Aroi	RA 9/9/2017	9/9/2017	P0	-27.0947	-109.374	S	F	RAFPOS

3. INSTRUMENTATION

For analysis we used four analytical techniques that are: inductively coupled plasma – mass spectrometry (ICP-MS; low and high resolution), ICP-quadrupole MS (ICP-MSQ), Ion Chromatography (IC) and HTC-RIMS (High Temperature Conversion Elemental Analyzer Isotope Ratio Mass Spectrometry). In the following paragraphs I will briefly describe the basic theory of this instrumentation.

3.1 Coupled Plasma – Mass Spectrometry (ICP-MS)

ICP-MS is one of the most sensitive and selective technique for rapid multi-elemental analysis of water soluble compounds. The main ICP-MS components are the sample introduction system, the inductively coupled plasma, the sampling interfaces; the ion lenses the mass analyzer, the ion detector and the data acquisition system. Figure 12 shows a schematic diagram of a typical ICP-MS. This technique uses plasma as the atomization and ionization source pure argon gas is used as it allows to ionize atoms, radicals, molecules and ions. Plasmas are characterized by their temperature, electron and ion densities.

In ICP-MS a magnetic field is produced by a high frequency generator that acts as energy source. In the plasma, positive and negative charges move independently, thus it becomes electrical conductive and it responds strongly to electromagnetic fields. Power is supplied to ICPs by radiofrequency generators, they degenerate alternating current at the required frequency. Analytical performance of ICP spectrometry is directly affected by the quality of the aerosol generation, as liquid dispersed into fine aerosols thus liquid samples were introduced by a peristaltic pump. These aerosols are carried into the core of the plasma by a carrier gas (argon). High temperature plasma is generated by radio frequency field. While passing through the different heating zones of the plasma torch, these liquid aerosols are dried into solid particles, and vaporized into gaseous state further, these gaseous state samples travel to the analytical zone of the plasma where they are atomized into ground-state atoms. After this these, atoms collide with the electrons and produce excited ions. These excited atoms enter in the interface region that includes the sample cone and the skimmer cone. Here, the positive ions are extracted and focused into a linear path by a series of electrostatic lenses and directed into a quadrupole or a magnetic sector field mass analyzer. The selected mass-to-charge ratios are transmitted into the

ion detector. These ions are collected and amplified by the electron multiplier assembly and transferred into data acquisition system.

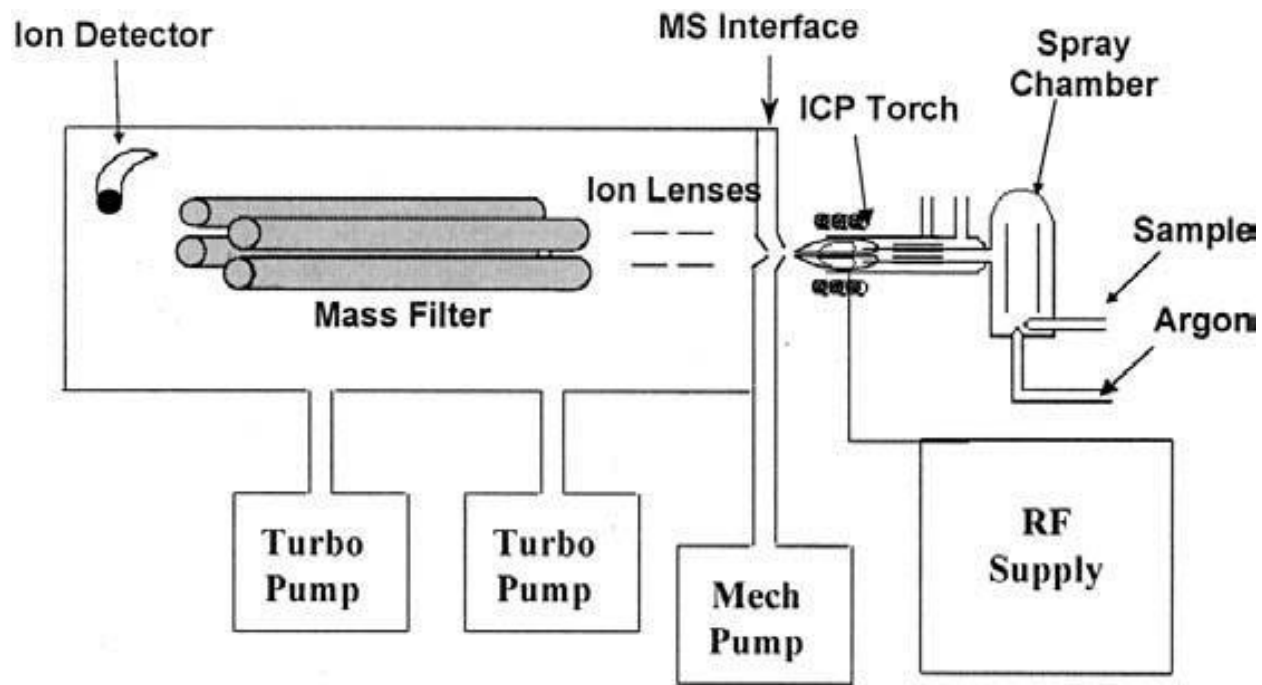


Figure 12: Shows schematic diagram of a typical ICP-MS setup
Source: (biochem.pepperdine.edu)

3.1.1 ICP-Quadrupole MS (ICP-MSQ)

The quadrupole mass filter is used to separate atoms with different m/z ratios. In this thesis I used a ICP coupled with a quadrupole mass spectrometer MSQ Plus, Thermo Fisher Scientific for the analysis of trace and rare earth elements.

Figure 13 shows the quadrupole mass analyzer system employed for the analysis. Mainly, the quadrupole consists of four rods where a combination of varying AC voltage operating at high frequency and DC voltage are applied. This voltage setting causes a rapid scanning of

elements with a unit mass resolution. This technique was used for determination of TE and REE in soil and filtrate obtain from water samples.

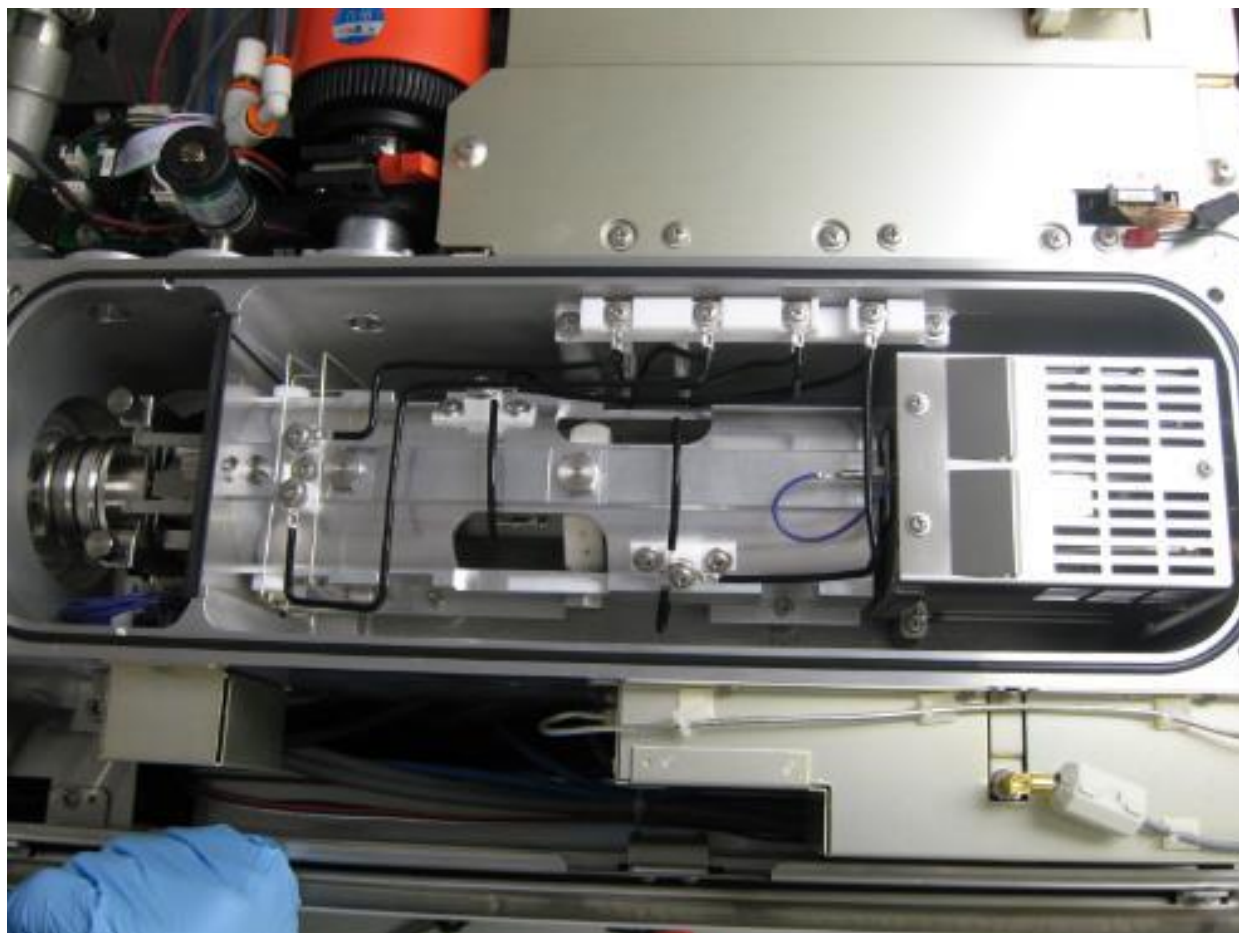


Figure 13: Quadrupole Mass Analyzer system of an ICP-MS

3.2 Ion Chromatography

Ion chromatography is used to identify, quantify and separates ions and polar molecules based on sample (mixture) affinity to the ion exchanger. This technique can be applied to separate any type of charged molecules like small nucleotides, amino acids, proteins etc. Anion exchange and cation exchange are main types of IC. When molecule of interest has positive charge cation exchange chromatography is employed, in principle stationary phase has negative

charge and solution with positive charges is loaded to be attracted to it. Similarly when molecule of interest is negatively charged anion exchange chromatography is used. In this case stationary phase has positive charge and negatively charged mobile phase solution is loaded.

A typical ion chromatography instrument consists of degasser, sampler, pumps, and a detector. Figure 14 shows picture of a typical instrument of IC. Small volume usually in microliters of sample mixture to be analyzed is injected into the mobile phase draining through the column. Then the pump forces the eluent along with sample through separator column. On the basis of specific physical interaction with stationary phase, sample's components move through the column at different velocities. After emergence of sample through it enters into the suppressor, that enhances the detection of ions of samples. Based on physical or chemical property of analyte conductive cells measure and monitor the electrical conductance of the sample ions, and finally transmit the signals to chromatography software. On the basis of retention time software identifies each analytic by integrating the peak height or peak area, and results are displayed as chromatogram.

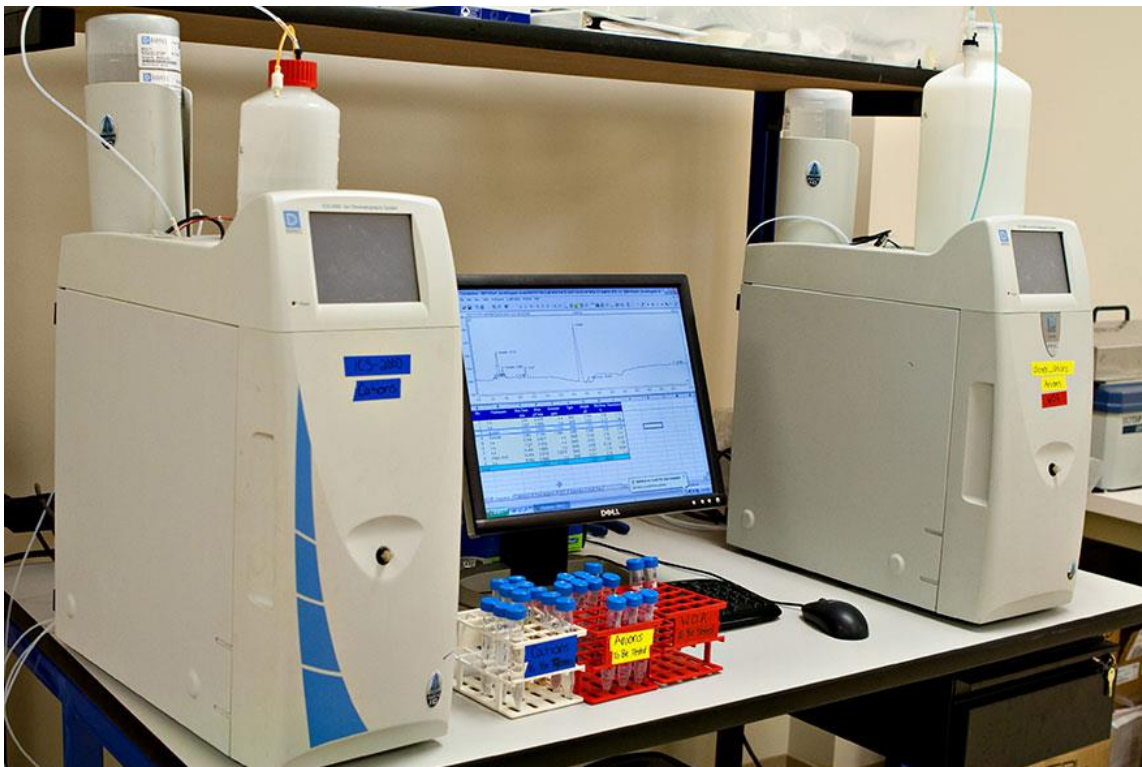


Figure 14: Picture of a typical instrument of Ion Chromatography

3.3 High Temperature Conversion Elemental Analyzer Isotope ratio mass spectrometry (HTC-RIMS)

This instrument measures small differences in the relative abundance of isotopes. Water can have large natural variations in isotope ratios of oxygen and hydrogen hence, for meaningful inter-laboratory comparisons of data normalization of stable isotope data is important. The isotopic analysis of oxygen and hydrogen isotopes can be divided into four steps: (a) elemental analyzer combustion or thermal conversion of the sample material (b) interface introduces the evolved gases into the ion source of mass spectrometer by ionization of gas molecules (c) The separation of the ions produces and (d) the detection of ions by using the mass spectrometer. Figure 15 shows the key components of typical HTC-RIMS.

In elemental analyzer system solid, low volatile liquids or liquids with low viscosity can directly inject by using a liquid inlet system. Then, in the combustion chamber, the temperature ranges between 1350 and 1450 °C and the sample is converted into H₂, N₂ and CO₂ gases. For the connection of IRMS and online elemental analyzer system interface is required. The interface dilutes the sample gas volume by addition of more helium gas and it limits the gas volume entering into the ion source and causes the introduction of pulses of working gas.

In mass spectrometer these gas molecules are ionized through the interaction between the electron beam and it pass through a magnetic field. The trajectory of the ions is determined by the strength of the magnetic field and accelerating voltage. Then multiple collectors simultaneously measure the ion intensity ratios.

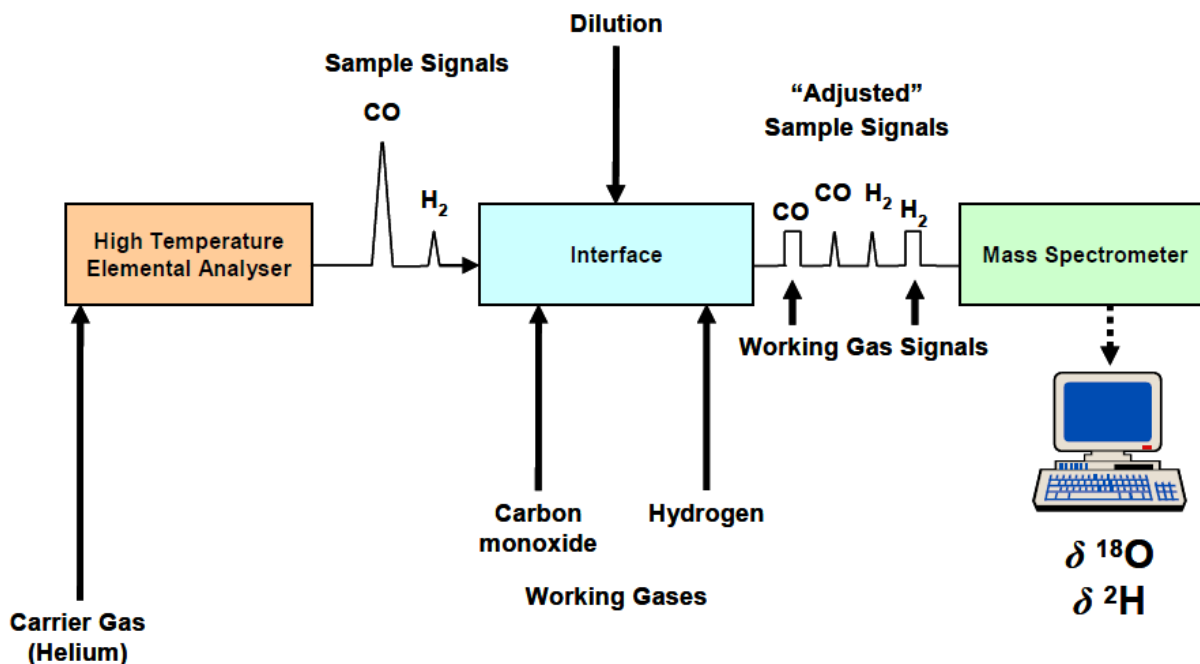


Figure 15: Systematic Diagram of HTC-RIMS Isotopic Analysis of O and H Isotopes
Source: www.biochem.pepperdine.edu

4. METHODOLOGY

Samples Preparation and Analysis

4.1 Analysis of trace and rare earth elements in water samples

The total concentration of selected trace and rare earth elements in water were analyzed with aICP-SFMS two days prior the water analysis, fresh standard solutions of RRE and TE were prepared at different concentrations. Rhodium (10 ppb) was used as internal standard in the ICP-MS analysis to correct possible instrumental variations. Water samples shortly before analysis were thawed and acidified with suprapur quality acid 1% v/v using an acidic solution consisting of 75% HNO₃ and 25% HCl. For analysis, ICP-SFMS was tuned and optimized according to manufacturer specifications and interferences were corrected.

4.2 Analysis of soil and filter samples:

Two duplicates from each dried soil samples were analyzed. These soil samples along with filter papers were treated under the same protocol to extract the trace elements (TE) and rare earth elements (REE). Filter papers and 30 mg of each soil sample were dissolved with 1.8 mL of HNO₃ and 2.4 mL of HF, and set for two days at room temperature in a clean environment. After two days, 20 mL of water was introduced in each test tube and kept at room temperature for six days. After six days, 24 mL water was added to reach a total of 50 mL final volume for each sample. After four days, all the metals were expected to be completely dissolved. Figure 16 shows these treated samples.

RRE and TE standard solutions of 5% nitric acid in low TOC water were prepared of different concentrations .These samples were analyzed using the ICP-MSQ.

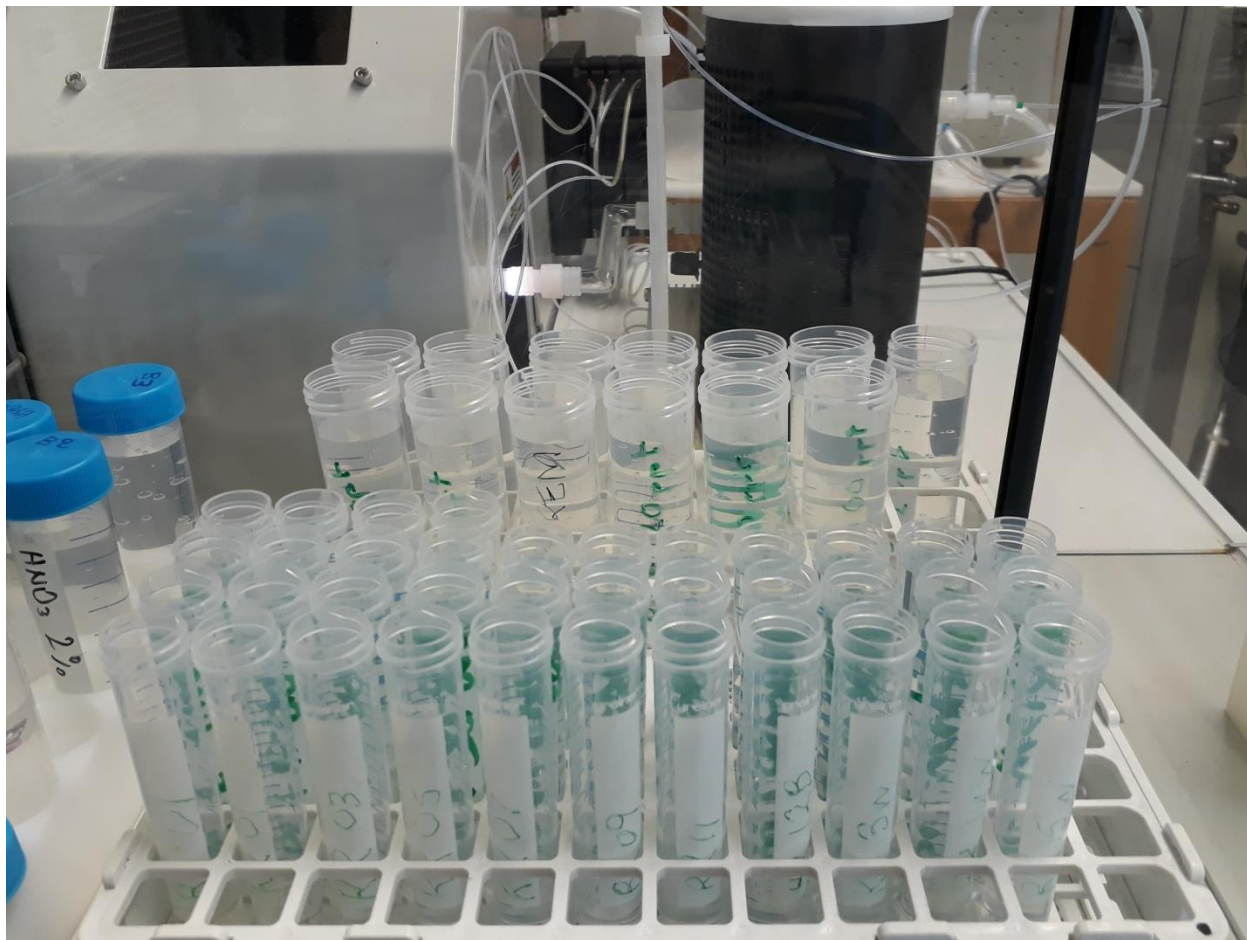


Figure 16: Soil and filter paper samples treated with HNO₃ and HF

4.3 Analysis of Cations and Anions in water samples

Ion chromatograph 883 Basic IC plus (Metrohm, Filderstadt, Germany) was used to analyze cations and anions concentration in the water samples. For the determination of cations a Metrosept 1-2 6.1010.000 column (4x125 mm, particulate size 7 μm) was used. The injection volume was 10 μL and 3mM HNO₃ was used as eluent. Similarly, for the analysis of anions a Metrosept anion supp/4 column was used (size 4x250 mm, particle size 5 μm). The injection volume was 20 μL and a flow of 0.7 mL min⁻¹ was used. The eluent used was 1.7 mM NaHCO₃ and 1.8mM Na₂CO₃.

Before analysis, when required, the samples were diluted with ultra-pure water at different concentrations, depending on the amount of ions that were present. Figure 17 shows the picture of diluted water samples at different concentrations. The quantification was performed using the external calibration method and standard solutions (Sigma Aldrich) at different concentrations (from 1 ppb to 10 ppm).

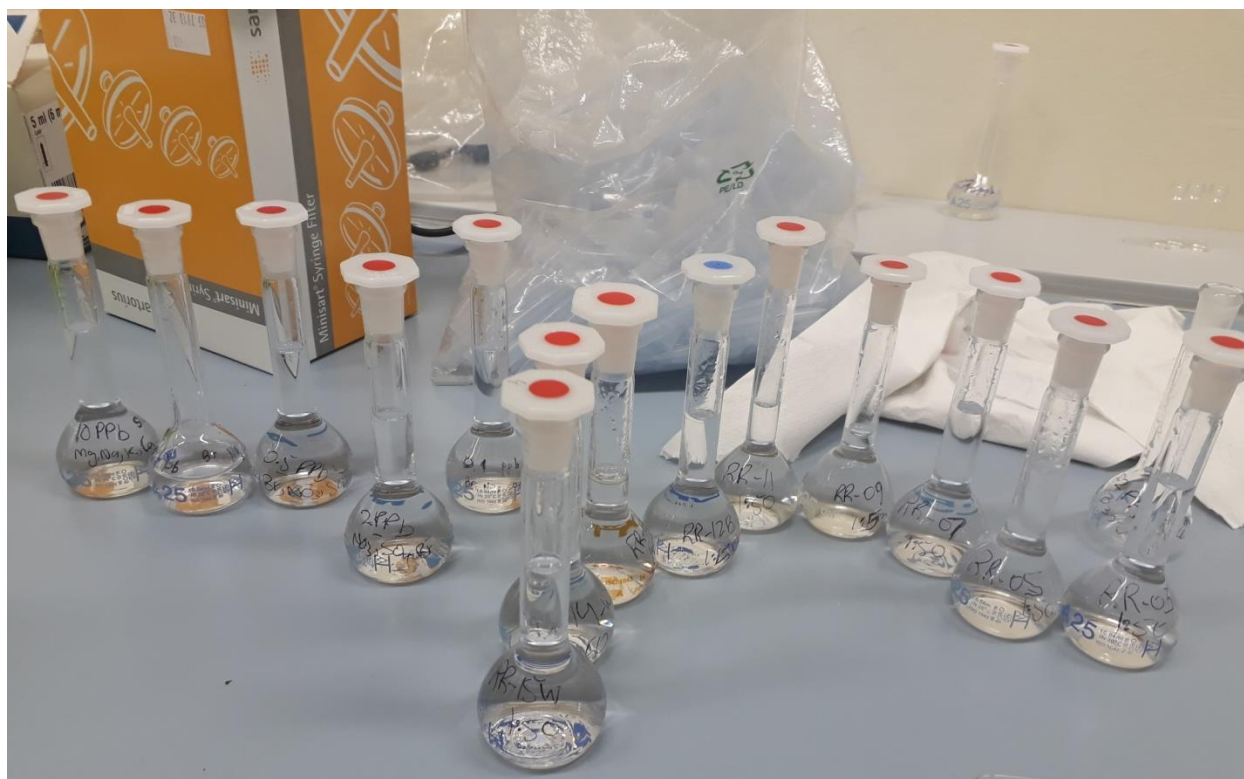


Figure 17: Diluted water samples of different concentration

4.4 Isotopic analysis of $\delta^{18}\text{O}$ and ^2H in water sample

Isotopic analysis of hydrogen and oxygen in the water samples was carried out in HTC-RIMS by using helium as carrier gas and the continuous flow method. Gas mixture of 0.3% CO_2 in helium with a purity of 99.996% were filled in vials and 500 μL sample water were injected

with a syringe through the membrane. For the equilibration of ^{18}O between CO_2 and H_2O , samples were kept closed for 24 hours.

Afterward, water samples were reduced by chromium to H_2 , and H_2 was then analyzed with the dual-inlet method without any carrier gas. Calibration was done with the three international standards named: Vienna Standard Mean Ocean Water (VSMOW), Standard light Antarctic Precipitation (SLAP) and Greenland Ice Sheet Precipitation (GISP).

4.5 Statistical analysis of the data

Enrichment factor and depletion factor of Rare earth element and trace element were calculated for Rano Raraku and Rano Aroi. Along with them fractional dynamics and cerium anomaly were also calculated. Following statistical tools were employed for calculation of these values

4.5.1 Equations used to calculate fractionation dynamics, ratio of LREE/HREE and Cerium anomaly

For the evaluation of fractionation dynamics, ratio of LREE/HREE was calculated using

Equation 1:

$$\frac{LREE}{HREE} = \frac{4(La_N + Pr_N + Nd_N)}{3(Er_N + Tm_N + Yb_N + Lu_N)}$$

Cerium Anomaly of soil and water of Rano Raraku and Rano roi was calculated by using

Equation 2:

$$Cerium\ Anomaly = \frac{\left[3 \left(\frac{Amount\ of\ Ce\ in\ the\ sample\ (\mu g\ l^{-1})}{Ce\ conc.(shale\ NASC)} \right) \right]}{\left[2 \left(\left(\frac{[Amount\ of\ La\ in\ Sample\ (\mu g\ l^{-1})]}{La\ conc.(shale\ NASC)} \right) + \left(\frac{[Amount\ of\ Nd\ in\ Sample\ (\mu g\ l^{-1})]}{Nd\ conc.(shale\ NASC)} \right) \right) \right]}$$

After the calculation of normalized values for rare earth elements and cerium anomaly following tests were employed to check possible outliers and normalized distribution of the data

Test-Q (Dixon)

Dixon test was used to individuate possible outliers in calculated ratio of LREE/HREE and cerium anomaly. Indeed, when Q-value calculated (Q_{calc}) exceeds the critical tabulated value (Q_{tab}) corresponding to the decided significance (95%, in this case), the suspected value can be rejected.

Following formula was used to calculate the results.

$$Q_n = \frac{|x_n - x_{n-1}|}{x_{max} - x_{min}}$$

If Q_n (for x_n) $> Q_{crit}$, then the value is an outlier. Q_{crit} depends on the number of samples ($Q_{crit, 95\%} = 0.625$ for $n=6$)

Shapiro-Wilk test

In order to check if the four groups; soil, water, filter and filter + water have (or not) normally distribution of values in LREE/HREE values and cerium anomaly, Shapiro-Wilk test was used. In this test W is a parameter very similar to the correlation coefficient. It varies from 0 to 1. 1 corresponds to an ideal normal distribution. The p-value represents the probability and p-values higher than 0.05 indicate that the distribution is normal at the 95% level.

F-test (Fisher)

In order to compare the mean values of LREE/HREE and cerium anomaly in the four matrices, it is necessary to assess the similarity of their variances. The comparison between the $F_{\text{calculated}} (S_1^2/S_2^2)$ and F_{critic} in conjunction with the corresponding p-value allow evaluating if the variance of the distribution is significantly similar or not. In particular, if $F_{\text{calc}} < F_{\text{crit}}$ the variances are homogeneous. The p-values > 0.05 ensure a homogeneity at a 95% level.

t-test (Student)

The t-test is used to assess if two means are significantly similar, t-values were calculated by using following formula:

$$t_{\text{calc}} = \frac{|\text{mean}(a) - \text{mean}(b)|}{S} \sqrt{\frac{n(a)n(b)}{n_a + n_b}}$$

Where (a) and (b) are the two means. S is the mean standard deviation and n is the size of the population. The t_{calc} is compared with the $t_{\text{tabulated}}$ for the corresponding degree of freedom (*df*) calculated with the Welch-Satterhwaite formula in the case of the in homogeneity of the variance for a certain confidence level (95% in this case; if p-value is higher than 0.05 the means are significantly (at 95%) similar). Then, if $t_{\text{calc}} < t_{\text{tab}}$ the means are significantly similar where the p-value explain this significance.

4.5.2 Calculation of enrichment factor and depletion factor

For calculation of enrichment factor (EF), that is measure of minimum factor of weight percent of the mineral (RRE and TE) present in the soil of Rano Raraku which is greater than the average occurrence of that mineral in the Earth's crust. Following formula was used.

$$EF = \frac{\frac{\text{Conc. of element in sampled soil } (\mu\text{g l}^{-1})}{\text{Conc. of Al in sampled soil } (\mu\text{g l}^{-1})}}{\frac{\text{Conc. of element in continental crust}}{\text{Conc. of Al in continental crust}}}$$

Similarly, depletion factor (DF) was also calculated to know how much soil is depleted in RRE and TE. For calculation of DF following formula was used that is reciprocal of EF.

$$DF = \frac{1}{EF}$$

5. RESULTS

5.1 Concentration of trace elements in Rano Raraku and Rano Aroi

Concentration of TE in the soil and filtrate samples were analyzed by MS (ICP-MSQ). Water sample analysis was carried out by ICP-MS. Table 4 shows thorough detail of TE concentration present in soil, filtrate and water samples.

As it is noticeable from the table, in RR aluminum and iron were present in high amount particularly high as in all the samples its concentration ranged from 105.39 to 149.05 mg g⁻¹ and 136.04 to 180.83 mg g⁻¹ respectively. Potassium, magnesium and calcium were also present in significant amount as their Concentration ranged between 2.62-8.49 mg g⁻¹, 4.10-13.46 mg g⁻¹ and 0.40-2.54 mg g⁻¹ respectively. It was observed TE were present in increasing concentration of Li<Be<Ag<Cs<Pb<V<Cr<Co<Ba<Cd<Cu<Ga<Sr<As<Na<Rb<Zn<Ca<Mn<K<Mg<Al<Fe.

As it is evident from Table 4 in filtrate of RR high amount of aluminum and iron were present that ranges between 171.05-911.47 µg l⁻¹ and 1783.95-467.12 µg l⁻¹ respectively. Cesium, lead, cobalt, nickel and silver are present in very less amount that was below 0.75, 0.22, 0.24, 0.41 and 0.18 µg l⁻¹ respectively. TE in RR were found in increasing concentration of Cd<Cs<Pb<Co<Ag<Ni<Ga<Be<Li<As<Sr<V<Ba<Zn<Na<K<Rb<Mn<Ca<Mg<Al<Fe.

It is evident from the Table 3 like RR in the RA aluminum and iron was present in greater concentration i-e 593.5 and 1910.68 µg l⁻¹ respectively. Unlike RR in filtrate of RA high amount of potassium was present that is 103.16 µg l⁻¹. In water samples of RR high amount of sodium was found i-e from 603 to 628 mg l⁻¹. Moreover, considerable high amount of potassium, magnesium and calcium were also detected in RR water samples their values ranged 21.86-

23.04, 52.46-53.74 and 14.10 to 14.93 mg l⁻¹ respectively. The order of increasing concentration of TE was found;

Be<Mn<Ag<Cs<Cd<Ga<Cr<Co<Al<Ni<V<Pb<Cu<As<Zn<Fe<Mn<Rb<Ba<Al,Sr<Ca<k<Mg<Na.

As it is evident from the Table 4 in the water samples of RA although it has high concentration of sodium i-e 35.39 mg l⁻¹ but it is very less as compare to RR water samples. Amount of potassium, magnesium and calcium was also found less than RR that was 0.76, 1.90 and 2.04 mg l⁻¹ respectively. Conversely, RR in the RA high amount of lead, nickel and cobalt were present their concentration was 1980.0, 732 and 747 µg l⁻¹ respectively. In RA TE were analyzed in increasing concentration of

Cs<Be<Ag<Mn<Cd<Cr<Li<Co<Pb<As<Cu<Ba<Zn<Sr<Mn<Al<Fe<K<Mg<Ca<Na.

Table 4: Trace element concentration in soil and water samples of Rano Raraku and Rano Aroi

		Li	Na	K	Rb	Cs	Be	Mg	Ca	Sr	Ba	
		$\mu\text{g g}^{-1}$	$\mu\text{g g}^{-1}$	mg g^{-1}	$\mu\text{g g}^{-1}$	$\mu\text{g g}^{-1}$	ng g^{-1}	mg g^{-1}	mg g^{-1}	$\mu\text{g g}^{-1}$	$\mu\text{g g}^{-1}$	
Soil	RR_S_P4_	16.68	40.55	2.66	208.39	0.38	7.94	7.02	1.01	25.27	282.25	
	RR_S_P5_A	16.60	276.12	8.49	231.99	0.34	6.75	6.78	0.46	16.61	234.71	
	RR_S_P5_B	13.85	77.55	4.93	208.02	0.29	6.29	4.10	0.40	21.12	220.94	
	RR_S_P6_A	15.79	59.48	5.60	226.02	0.37	5.71	4.51	0.86	18.07	191.76	
	RR_S_P6_B	16.62	268.75	6.52	219.79	0.29	5.95	4.64	0.73	16.19	162.41	
	RR_S_P7_	13.17	46.60	2.82	233.75	0.47	6.23	13.46	2.54	53.12	191.09	
Raraku	Filter	RR_F_P1_S	$\mu\text{g l}^{-1}$ 0.71	$\mu\text{g l}^{-1}$ 10.07	$\mu\text{g l}^{-1}$ 27.51	$\mu\text{g l}^{-1}$ 12.24	$\mu\text{g l}^{-1}$ 0.027	$\mu\text{g l}^{-1}$ 0.22	$\mu\text{g l}^{-1}$ 106.66	$\mu\text{g l}^{-1}$ 56.96	$\mu\text{g l}^{-1}$ 1.21	$\mu\text{g l}^{-1}$ 2.29
		RR_F_P2_S	0.90	15.16	15.20	17.22	0.022	0.34	112.35	37.57	1.16	1.03
		RR_F_P3_S	0.89	10.35	11.46	16.83	0.018	0.34	93.56	34.26	1.09	1.21
		RR_F_P1_90	1.00	18.20	14.91	19.86	0.017	0.42	180.95	71.06	2.26	3.33
		RR_F_P2_51	0.91	21.57	16.31	19.83	0.016	0.42	241.77	107.84	2.94	3.60
		RR_F_P3_38	0.72	13.99	13.37	16.23	0.012	0.34	127.96	48.86	1.59	1.79
Water	RR_W_P1_S	ng l^{-1} 201.34	mg l^{-1} 606.60	mg l^{-1} 22.31	$\mu\text{g l}^{-1}$ 20.10	ng l^{-1} 6.74	ng l^{-1} 3.09	mg l^{-1} 52.49	mg l^{-1} 14.93	$\mu\text{g l}^{-1}$ 693.81	$\mu\text{g l}^{-1}$ 30.34	
	RR_W_P2_S	84.02	604.05	23.04	13.54	5.82	2.93	53.46	14.91	493.09	19.78	
	RR_W_P1_90	139.37	608.50	21.86	14.00	5.90	2.62	53.74	14.81	521.09	20.25	
	RR_W_P2_51	75.21	628.60	22.41	18.15	5.73	1.86	53.31	14.50	726.82	28.66	
	RR_W_P3_38	73.18	613.55	21.96	16.49	5.66	1.66	52.03	14.10	572.15	22.44	
	RR_W_P3_S	90.55	603.40	22.11	20.08	5.54	2.36	52.70	14.53	726.38	27.78	
Aroi	Filter	$\mu\text{g l}^{-1}$ 3.17	$\mu\text{g l}^{-1}$ 9.50	$\mu\text{g l}^{-1}$ 103.16	$\mu\text{g l}^{-1}$ 59.77	$\mu\text{g l}^{-1}$ 0.16	$\mu\text{g l}^{-1}$ 1.01	$\mu\text{g l}^{-1}$ 69.81	$\mu\text{g l}^{-1}$ 52.09	$\mu\text{g l}^{-1}$ 1.15	$\mu\text{g l}^{-1}$ 0.50	
	Water	ng l^{-1} 204.88	mg l^{-1} 35.39	mg l^{-1} 0.76	$\mu\text{g l}^{-1}$ 0.34	ng l^{-1} 3.06	ng l^{-1} 4.68	mg l^{-1} 1.98	mg l^{-1} 2.04	$\mu\text{g l}^{-1}$ 26.74	$\mu\text{g l}^{-1}$ 2.25	

Table 1 (continued)

		Al	Fe	Mn	V	Cr	Ag	Cd	Pb	Co	Ni	Cu	Zn	Ga	As	
		mg g ⁻¹	mg g ⁻¹	mg g ⁻¹	µg g ⁻¹	µg g ⁻¹	ng g ⁻¹	ng g ⁻¹	µg g ⁻¹	µg g ⁻¹	µg g ⁻¹	µg g ⁻¹	µg g ⁻¹	µg g ⁻¹	µg g ⁻¹	
Raraku	Soil	RR_S_P4_	137.60	141.54	2.54	4.98	59.84	1.60	72.54	1.78	40.94	4.05	21.70	271.59	70.04	11.59
		RR_S_P5_A	143.19	180.83	2.82	6.37	91.51	1.52	77.41	1.53	49.92	5.91	54.73	303.22	72.10	13.26
		RR_S_P5_B	141.77	151.90	2.34	6.54	73.88	1.69	77.83	1.67	38.44	4.98	34.50	270.73	68.40	11.95
		RR_S_P6_A	142.80	148.96	3.88	3.74	58.68	1.46	72.82	1.60	44.62	4.37	36.26	232.93	63.65	10.35
		RR_S_P6_B	149.05	137.59	2.28	1.84	42.42	1.53	78.46	1.54	80.05	4.54	52.26	253.86	62.93	7.89
		RR_S_P7_	105.39	136.04	2.23	3.10	47.00	1.22	57.47	1.42	36.45	6.69	22.44	206.94	53.30	10.40
Raraku	Filter	RR_F_P1_S	µg l ⁻¹ 257.41	µg l ⁻¹ 543.93	µg l ⁻¹ 36.44	µg l ⁻¹ 1.70	µg l ⁻¹ 5.71	µg l ⁻¹ 0.18	µg l ⁻¹ 0.009	µg l ⁻¹ 0.10	µg l ⁻¹ 0.13	µg l ⁻¹ 0.25	µg l ⁻¹ 0.67	µg l ⁻¹ 4.14	µg l ⁻¹ 0.29	µg l ⁻¹ 1.12
		RR_F_P2_S	171.05	458.27	45.33	1.61	5.82	0.06	0.010	0.05	0.13	0.25	0.79	3.43	0.17	1.34
		RR_F_P3_S	183.02	467.12	45.61	1.60	5.73	0.05	0.011	0.04	0.13	0.21	0.75	3.14	0.19	1.23
		RR_F_P1_90	562.84	1323.98	75.06	2.05	6.58	0.06	0.016	0.20	0.24	0.41	0.97	6.29	0.49	1.14
		RR_F_P2_51	911.47	1783.95	81.68	2.43	7.20	0.06	0.020	0.22	0.38	0.35	1.12	6.18	0.63	1.27
		RR_F_P3_38	304.60	789.99	62.38	2.18	7.24	0.05	0.014	0.06	0.19	0.27	0.81	4.01	0.27	1.27
Raraku	Water	RR_W_P1_S	µg l ⁻¹ 64.87	µg l ⁻¹ 2.65	µg l ⁻¹ 20.59	ng l ⁻¹ 110.34	ng l ⁻¹ 82.34	ng l ⁻¹ 9.83	ng l ⁻¹ 38.31	ng l ⁻¹ 161.13	ng l ⁻¹ 79.32	ng l ⁻¹ 215.66	µg l ⁻¹ 1.00	µg l ⁻¹ 2.37	ng l ⁻¹ 34.20	µg l ⁻¹ 1.25
		RR_W_P2_S	52.41	1.74	2.94	96.47	49.87	2.97	26.86	127.69	71.11	104.76	0.67	1.39	36.50	1.22
		RR_W_P1_90	52.28	2.70	2.39	181.70	66.44	5.00	33.62	112.91	76.06	113.84	0.60	1.25	42.49	1.30
		RR_W_P2_51	79.54	4.68	13.72	148.00	64.36	1.68	45.70	167.64	77.14	82.20	0.49	1.68	39.32	1.19
		RR_W_P3_38	62.24	1.62	3.01	109.21	55.24	1.89	28.96	120.37	70.27	104.60	0.50	1.08	39.98	1.09
		RR_W_P3_S	73.42	1.59	5.28	100.66	53.69	2.55	26.96	103.65	74.47	110.06	0.87	1.19	37.07	1.23
Aroi	Filter	RA_F_P0_S	µg l ⁻¹ 593.56	µg l ⁻¹ 1910.68	µg l ⁻¹ 4.86	µg l ⁻¹ 6.17	µg l ⁻¹ 26.09	µg l ⁻¹ 0.48	µg l ⁻¹ 0.04	µg l ⁻¹ 1.05	µg l ⁻¹ 0.47	µg l ⁻¹ 1.05	µg l ⁻¹ 10.90	µg l ⁻¹ 16.19	µg l ⁻¹ 0.59	µg l ⁻¹ 5.77
		Water RA_W_P0_S	µg l ⁻¹ 151.90	µg l ⁻¹ 701.98	µg l ⁻¹ 31.00	ng l ⁻¹ 698.17	ng l ⁻¹ 347.13	ng l ⁻¹ 10.43	ng l ⁻¹ 58.73	ng l ⁻¹ 1980.00	ng l ⁻¹ 732.21	ng l ⁻¹ 747.94	µg l ⁻¹ 2.21	µg l ⁻¹ 11.23	ng l ⁻¹ n.a.	µg l ⁻¹ 1.07

5.2 Concentration of rare earth elements in Rano Raraku and Rano Aroi

In the soil samples from RR concentration of RRE in $\mu\text{g g}^{-1}$ are shown in Table 5. Obtained results shows that cerium have comparatively high amount that is 29.9 to 45.3 $\mu\text{g g}^{-1}$. As it is evident from the results lutetium, thulium, holmium and terbium were present in low concentration as their average concentration found was 0.2, 0.23, 0.58 and 0.45 respectively. In RR rare earth elements were found present in decreasing concentration order as $\text{Ce} > \text{Nd} > \text{La} > \text{Dy} > \text{Gd} > \text{Pr} > \text{Sm} > \text{Er} > \text{Yb} > \text{Eu} > \text{Ho} > \text{Tb} > \text{Tm} > \text{Lu}$.

Detail values of concentration of RRE in RR shown in Table 5. It was observed in the water sample of RR cerium concentration was found in high amount; as its value ranged from 2.48 to 5.87 $\mu\text{g g}^{-1}$. Water samples from RR have decreasing order of concentration of RRE $\text{Nd} > \text{La} > \text{Sm} > \text{Yb} > \text{Dy} > \text{Er} > \text{Gd} > \text{Pr} > \text{Eu} > \text{Ho} > \text{Lu} > \text{Tb} > \text{Tm}$. Similarly in RA water sample cerium concentration was also found in high amount that was 110.31 $\mu\text{g g}^{-1}$. As it is evident from the Table 5 in RA decreasing concentration of RRE was

$\text{Nd} > \text{La} > \text{Sm} > \text{Dy} > \text{Gd} > \text{Pr} > \text{Er} > \text{Yb} > \text{Eu} > \text{Ho} > \text{Lu} > \text{Tm}$.

Table 5 shows detail of abundance of RRE in RR and RA filtrate samples. As it is evident from calculated amount obtained from filtrate of RR cerium and lanthanide have comparatively greater concentration than rest of the RRE; cerium concentration ranged from 7.6 to 20.1 $\mu\text{g g}^{-1}$ and lanthanide 3.6 to 10.0 $\mu\text{g g}^{-1}$. While in RA filtrate sample concentration of cerium and lanthanide was 6.9 and 3.6 $\mu\text{g g}^{-1}$ respectively. RRE were present in RR and RA in increasing order of $\text{Lu} < \text{Yb} < \text{Tm} < \text{Er} < \text{Ho} < \text{Tb} < \text{Gd} < \text{Eu} < \text{Sm} < \text{Dy} < \text{Pr}$.

Higher rare earth elements (HREE) La, Pr and Nd normalized value concentration in soil sample ranges from 3.00 to 9.53 while lower rare earth elements (LREE) Er, Tm, Yb and Lu normalized value ranges from 0.96 to 3.98.

Table 5: Rare earth element concentration in soil and water samples of Rano Raraku and Rano Aroi

		La	Ce	Pr	Nd	Sm	Eu	Gd	Tb	Dy	Ho	Er	Tm	Yb	Lu
		$\mu\text{g l}^{-1}$	$\mu\text{g l}^{-1}$	$\mu\text{g l}^{-1}$	$\mu\text{g l}^{-1}$	$\mu\text{g l}^{-1}$	$\mu\text{g l}^{-1}$	$\mu\text{g l}^{-1}$	$\mu\text{g l}^{-1}$	$\mu\text{g l}^{-1}$	$\mu\text{g l}^{-1}$	$\mu\text{g l}^{-1}$	$\mu\text{g l}^{-1}$	$\mu\text{g l}^{-1}$	$\mu\text{g l}^{-1}$
Soil	RR_S_P4_	7.85	39.23	2.90	10.04	2.60	1.20	3.39	0.76	4.05	1.01	2.53	0.40	2.04	0.36
	RR_S_P5_A	5.57	44.53	2.01	6.84	1.68	0.75	2.11	0.47	2.53	0.63	1.59	0.25	1.30	0.22
	RR_S_P5_B	5.18	45.26	1.91	6.49	1.64	0.73	2.04	0.46	2.46	0.61	1.54	0.25	1.27	0.22
	RR_S_P6_A	2.14	31.11	1.07	3.87	1.06	0.47	1.23	0.27	1.41	0.34	0.84	0.14	0.71	0.12
	RR_S_P6_B	1.47	35.93	0.73	2.66	0.78	0.36	1.00	0.23	1.24	0.30	0.76	0.13	0.66	0.12
	RR_S_P7_	7.56	29.85	2.57	8.56	1.96	0.84	2.27	0.49	2.47	0.59	1.40	0.22	1.05	0.18
			$\mu\text{g g}^{-1}$	$\mu\text{g g}^{-1}$	$\mu\text{g g}^{-1}$	$\mu\text{g g}^{-1}$	$\mu\text{g g}^{-1}$	$\mu\text{g g}^{-1}$	$\mu\text{g g}^{-1}$	$\mu\text{g g}^{-1}$	$\mu\text{g g}^{-1}$	$\mu\text{g g}^{-1}$	$\mu\text{g g}^{-1}$	$\mu\text{g g}^{-1}$	$\mu\text{g g}^{-1}$
Raraku	RR_F_P1_S	27.56	60.28	8.38	26.57	5.34	2.64	6.12	1.50	5.92	1.71	3.45	0.81	2.52	0.74
	RR_F_P2_S	18.90	40.25	5.74	18.17	3.72	2.05	4.08	1.32	4.07	1.49	2.52	0.80	1.78	0.82
	RR_F_P3_S	18.88	39.96	6.15	19.25	3.70	2.07	4.26	1.42	4.28	1.56	2.76	0.86	1.91	0.83
	RR_F_P1_90	57.13	126.27	18.66	60.68	13.07	5.99	14.28	3.37	13.66	3.80	8.04	1.72	5.84	1.59
	RR_F_P2_51	91.29	214.70	28.19	92.62	20.13	8.97	21.71	4.78	20.64	5.49	11.93	2.31	8.46	2.14
	RR_F_P3_38	33.22	70.87	10.84	35.27	7.52	3.60	8.13	2.11	8.02	2.41	4.95	1.16	3.56	1.14
			$\mu\text{g g}^{-1}$	$\mu\text{g g}^{-1}$	$\mu\text{g g}^{-1}$	$\mu\text{g g}^{-1}$	$\mu\text{g g}^{-1}$	$\mu\text{g g}^{-1}$	$\mu\text{g g}^{-1}$	$\mu\text{g g}^{-1}$	$\mu\text{g g}^{-1}$	$\mu\text{g g}^{-1}$	$\mu\text{g g}^{-1}$	$\mu\text{g g}^{-1}$	$\mu\text{g g}^{-1}$
Water	RR_W_P1_S	2.99	4.13	0.91	4.03	3.43	0.90	1.60	0.28	1.98	0.55	1.81	0.33	2.26	0.48
	RR_W_P2_S	2.90	4.72	0.74	3.30	3.10	0.93	1.36	0.27	1.77	0.53	1.55	0.29	1.96	0.42
	RR_W_P1_90	7.46	5.87	1.78	7.89	5.58	1.22	2.50	0.47	2.93	0.76	2.44	0.34	2.63	0.54
	RR_W_P2_51	1.99	2.86	0.57	2.57	2.21	0.72	1.01	0.22	1.50	0.42	1.49	0.25	1.87	0.41
	RR_W_P3_38	2.10	2.97	0.65	2.84	2.99	0.86	1.15	0.24	1.63	0.50	1.64	0.29	1.89	0.42
	RR_W_P3_S	1.74	2.48	0.57	2.57	2.24	0.79	1.01	0.23	1.44	0.44	1.42	0.24	1.78	0.40
			$\mu\text{g g}^{-1}$	$\mu\text{g g}^{-1}$	$\mu\text{g g}^{-1}$	$\mu\text{g g}^{-1}$	$\mu\text{g g}^{-1}$	$\mu\text{g g}^{-1}$	$\mu\text{g g}^{-1}$	$\mu\text{g g}^{-1}$	$\mu\text{g g}^{-1}$	$\mu\text{g g}^{-1}$	$\mu\text{g g}^{-1}$	$\mu\text{g g}^{-1}$	$\mu\text{g g}^{-1}$
Aroi	Filter RA_F_P0_S	22.10	41.69	5.56	10.83	1.12	1.81	1.14	1.84	2.33	1.97	1.98	1.49	0.81	1.62
	Water RA_W_P0_S	40.40	110.31	15.78	58.78	37.92	5.77	18.25	2.92	18.19	3.62	10.22	1.49	9.15	1.52

5.3 Ions analysis of water samples of Rano Raraku and Rano Aroi

Anions and cations analysis was performed on water samples by using ion chromatography. Table 6 shows the comprehensive detail of ion concentrations found in water samples.

As is evident from the table, in Rano Raraku, chloride ions were particularly high as in all the samples its concentration ranged from 952 to 991 ppm. Concentrations of nitrites and nitrates were not found significantly high as they were below 0.3 and 0.2 ppm, respectively. Ammonium and bromide concentrations ranged between 3-7 ppm and between 3.5-3.7 ppm, respectively. Values for sulphate ions are below 1.1 ppm, except for RR-W-P2-51 that is slightly higher (2.1 ppm).

In Rano Aroi, chloride concentration is significantly lower (58 ppm) than in Rano Raraku. Similarly, nitrites, ammonium and bromides are lower than RR. Conversely, nitrates resulted higher (1.9 ppm). Sulphate concentration is similar, although slightly lower.

Table 6: Presence of cations and anions in water samples of Rano Raraku and Rano Aroi

	NH4	Cl	NO2	Br	NO3	SO4
	ppm	ppm	ppm	ppm	ppm	ppm
RA_W_P0_S	0.20	58.36	0.00	0.12	1.93	0.42
RR_W_P1_S	5.19	990.72	0.25	3.55	0.19	1.01
RR_W_P2_S	5.35	952.30	0.27	3.61	0.10	0.79
RR_W_P1_90	3.16	959.62	0.31	3.62	0.09	1.12
RR_W_P2_51	6.89	991.13	0.16	3.64	0.11	2.11
RR_W_P3_38	3.35	967.90	0.30	3.63	0.06	0.79
RR_W_P3_S	6.12	955.74	0.30	3.63	0.13	0.80

5.4 Isotopic Analysis

The isotopic enrichment of $\delta^{18}\text{O}$, δD and the d-excess (d). This latter (d) is defined as The deuterium excess, defined as $d = \delta\text{D} - \delta^{18}\text{O}$ (where δD and $\delta^{18}\text{O}$ denote the deuterium and

oxygen-18 abundance relative to VSMOW – Vienna Standard Mean Ocean Water), the values obtained from RR and RA water samples are shown in Table 7. As is evident in RR water samples the isotopic enrichment values are quite constant as δD ranges from 22.7 to 26.4 ‰, and $\delta^{18}O$ was between 3.97 to 4.10. The calculated deuterium excess were from -9.79 to -9.07 ‰. Conversely, RA water samples showed negative values of $\delta^{18}O$ and δD (i.e. -2.92 and -7.15 respectively), while d-excess calculated value was 16.22 ‰.

Table 7: Isotopic enrichment of $\delta^{18}O$, δD and d-excess values of water samples.

#Name	δD	$\delta^{18}O$	d-excess
RA_W_P0_S	-7.15	-2.92	16.22
RR_W_P1_S	25.10	3.99	-6.79
RR_W_P2_S	25.21	4.10	-7.55
RR_W_P1_90	22.72	3.97	-9.03
RR_W_P2_51	24.66	3.97	-7.09
RR_W_P3_38	23.57	3.97	-8.21
RR_W_P3_S	26.36	4.07	-6.19

5.5.1 Enrichment factors

Abundance of rare earth elements and trace elements found in upper crust of the earth surface reported in Composition of the Continental Crust. Treatise Geochem 3:1-64 are used as reference values to compare my obtained values in soil samples collected from RR soil samples by using analytic technique of ICP-MSQ. Table 8 shows the detail Enrichment factors (EF) values of RRE and TE found in soil samples, aluminum concentration value was used to normalize results.

From the results it can be observe that values of RRE Lanthanum to Lutetium are not significantly high. However, value of Manganese shows high EF ranging from 24.48 to 36.3 in sample RR-S-P6-B and RR-S-P6-A respectively. On second number high trend of silver EF was observed from 15.69 to 17.89. Zinc, iron and gallium concentration were also found slightly high from 3.7 to 2.07 EF. Figure 18 shows the trend of EF in bar graph.

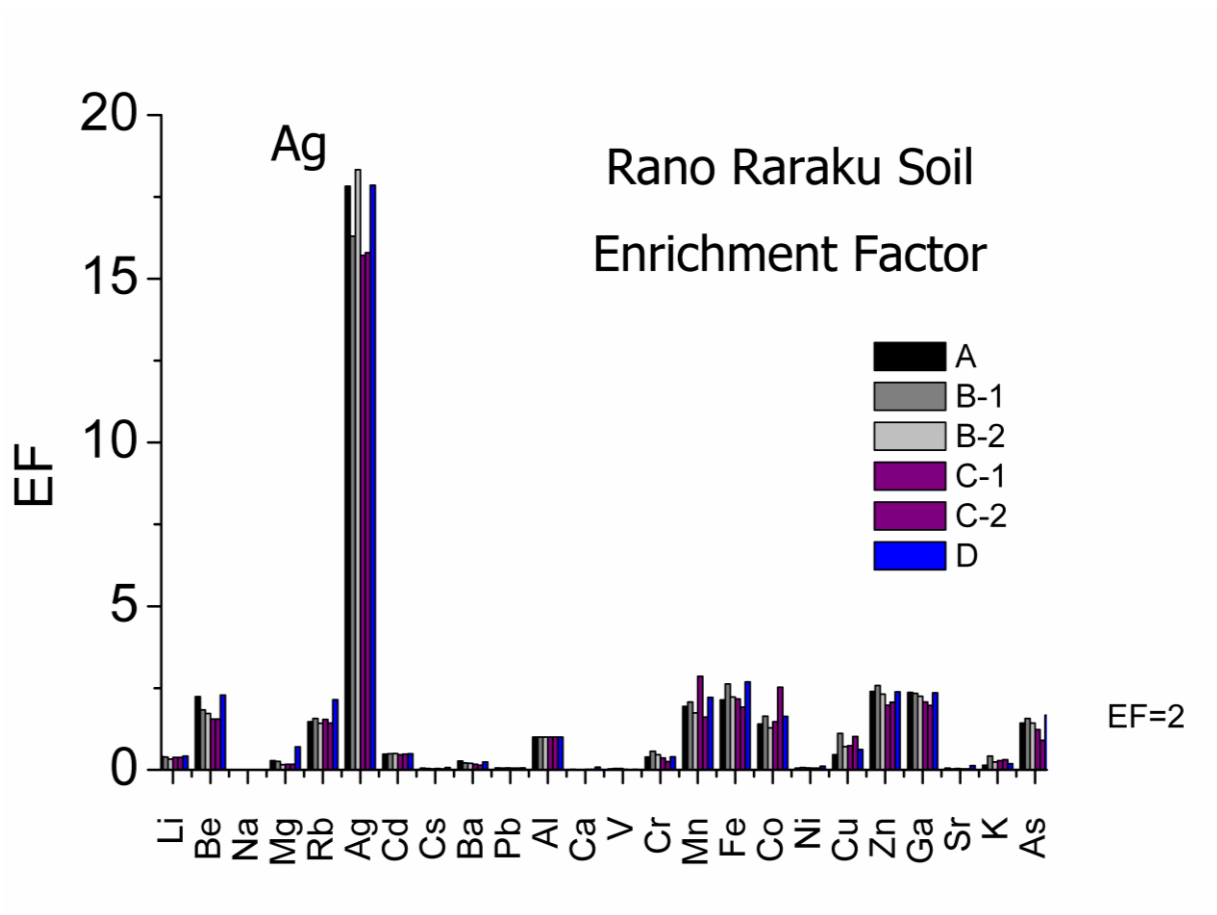


Figure 18: Enrichment Factor values of Rare earth elements and trace elements found in Rano Raraku

Table 8: Enrichment Factor values of Rare earth elements and trace elements found in Rano Raraku

	Li	Be	Na	Mg	Rb	Ag	Cd	Cs	Ba	Pb	Al	Ca
	EF (Al)	EF (Al)	EF (Al)	EF (Al)	EF (Al)	EF (Al)	EF (Al)	EF (Al)	EF (Al)	EF (Al)	EF (Al)	EF (Al)
RR_S_P4_	0.41	2.24	0.00	0.28	1.47	17.83	0.48	0.05	0.27	0.06	1.00	0.02
RR_S_P5_A	0.39	1.83	0.01	0.26	1.57	16.30	0.49	0.04	0.21	0.05	1.00	0.01
RR_S_P5_B	0.33	1.72	0.00	0.16	1.42	18.33	0.50	0.03	0.20	0.06	1.00	0.01
RR_S_P6_A	0.38	1.55	0.00	0.17	1.54	15.71	0.46	0.04	0.17	0.05	1.00	0.02
RR_S_P6_B	0.38	1.55	0.01	0.17	1.43	15.79	0.48	0.03	0.14	0.05	1.00	0.02
RR_S_P7_	0.42	2.29	0.00	0.70	2.15	17.86	0.49	0.07	0.24	0.06	1.00	0.08

	V	Cr	Mn	Fe	Co	Ni	Cu	Zn	Ga	Sr	K	As
	EF (Al)	EF (Al)	EF (Al)	EF (Al)	EF (Al)	EF (Al)	EF (Al)	EF (Al)	EF (Al)	EF (Al)	EF (Al)	EF (Al)
RR_S_P4_	0.03	0.39	1.94	2.14	1.40	0.05	0.46	2.40	2.37	0.05	0.14	1.43
RR_S_P5_A	0.04	0.57	2.08	2.63	1.64	0.07	1.11	2.58	2.34	0.03	0.42	1.57
RR_S_P5_B	0.04	0.46	1.74	2.23	1.28	0.06	0.71	2.32	2.25	0.04	0.24	1.43
RR_S_P6_A	0.02	0.36	2.86	2.17	1.47	0.05	0.74	1.98	2.08	0.03	0.28	1.23
RR_S_P6_B	0.01	0.25	1.61	1.92	2.53	0.05	1.02	2.07	1.97	0.03	0.31	0.90
RR_S_P7_	0.02	0.40	2.22	2.69	1.63	0.11	0.62	2.39	2.36	0.13	0.19	1.67

	La	Ce	Pr	Nd	Sm	Eu	Gd	Tb	Dy	Ho	Er	Tm	Yb	Lu
	EF (Al)	EF (Al)	EF (Al)	EF (Al)	EF (Al)	EF (Al)	EF (Al)	EF (Al)	EF (Al)	EF (Al)	EF (Al)	EF (Al)	EF (Al)	EF (Al)
RR_S_P4_	0.15	0.37	0.24	0.22	0.33	0.71	0.50	0.64	0.61	0.72	0.65	0.78	0.62	0.70
RR_S_P5_A	0.10	0.40	0.16	0.14	0.20	0.43	0.30	0.38	0.37	0.43	0.39	0.48	0.38	0.41
RR_S_P5_B	0.10	0.41	0.15	0.14	0.20	0.42	0.29	0.38	0.36	0.42	0.39	0.47	0.37	0.41
RR_S_P6_A	0.04	0.28	0.09	0.08	0.13	0.27	0.18	0.22	0.21	0.23	0.21	0.26	0.21	0.23
RR_S_P6_B	0.03	0.31	0.06	0.05	0.09	0.20	0.14	0.18	0.17	0.20	0.18	0.23	0.18	0.20
RR_S_P7_	0.19	0.37	0.28	0.25	0.32	0.65	0.44	0.55	0.49	0.55	0.47	0.56	0.41	0.44

5.5.2 Depletion factor

Depletion of rare earth elements and trace elements in soil sample of RR were calculated by division of EF value by 1. Table 9 shows the detail of depletion factor (DF) values of RRE and TE found in soil samples.

Results of DF calculated values show that RR soil is found to be deficient in many elements. Many TE have DF values specially sodium its value ranges from 154.35 to 1009.92. Magnesium, cesium, lead, calcium, vanadium, nickel and strontium also have significant high DF. They have values ranging from 1.43 to 6.32, 13.40 to 29.25, 15.50 to 20.14, 13.08 to 110.65, 96.40 to 25.82, 9.09 to 19.60 and 7.79 to 36.14 respectively.

From the results it is observed values of RRE has significant DF; prominently lanthanum, neodymium and praseodymium. Their values range from 5.30 to 38.62, 3.58 to 17.84 and 4.08 to 18.57 respectively. Figure 19 shows the trend of DF values of RRE and TE.

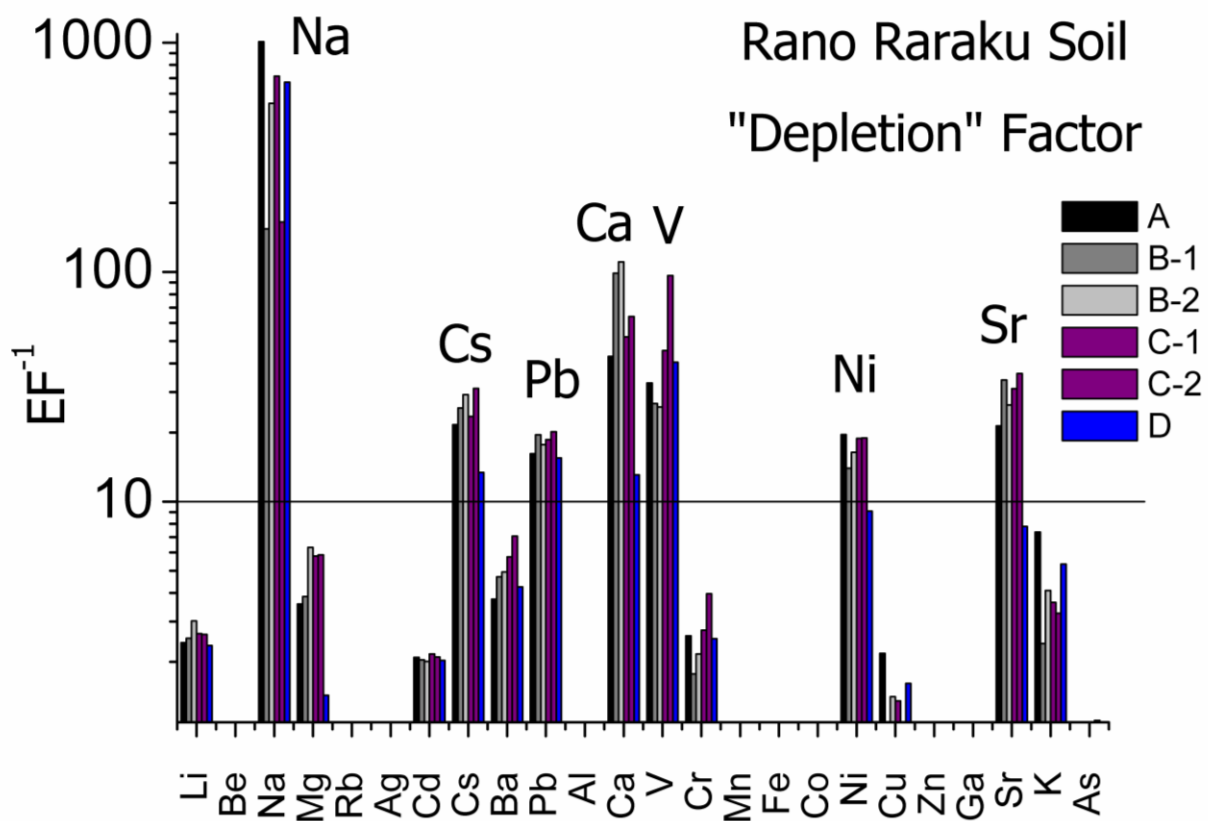


Figure 19: Trend of "Depletion factor" of rare earth elements and trace elements in Rano Raraku

Table 9: Depletion factor of rare earth elements and trace elements in Rano Raraku

	Li	Be	Na	Mg	Rb	Ag	Cd	Cs	Ba	Pb	Al	Ca
	DF (Al)	DF (Al)	DF (Al)	DF (Al)	DF (Al)	DF (Al)	DF (Al)	DF (Al)	DF (Al)	DF (Al)	DF (Al)	DF (Al)
RR_S_P4_	2.43	0.45	1009.92	3.58	0.68	0.06	2.09	21.63	3.76	16.15	1.00	42.94
RR_S_P5_A	2.54	0.55	154.35	3.86	0.64	0.06	2.04	25.58	4.70	19.54	1.00	98.80
RR_S_P5_B	3.02	0.58	544.11	6.32	0.70	0.05	2.01	29.25	4.94	17.71	1.00	110.65
RR_S_P6_A	2.66	0.64	714.62	5.79	0.65	0.06	2.17	23.49	5.74	18.63	1.00	52.23
RR_S_P6_B	2.64	0.65	165.08	5.86	0.70	0.06	2.10	31.14	7.07	20.14	1.00	64.04
RR_S_P7_	2.36	0.44	673.12	1.43	0.46	0.06	2.03	13.40	4.25	15.50	1.00	13.08

	V	Cr	Mn	Fe	Co	Ni	Cu	Zn	Ga	Sr	K	As
	DF (Al)	DF (Al)	DF (Al)	DF (Al)	DF (Al)	DF (Al)	DF (Al)	DF (Al)	DF (Al)	DF (Al)	DF (Al)	DF (Al)
RR_S_P4_	32.86	2.60	0.52	0.47	0.71	19.60	2.18	0.42	0.42	21.38	7.37	0.70
RR_S_P5_A	26.75	1.77	0.48	0.38	0.61	13.97	0.90	0.39	0.43	33.86	2.41	0.64
RR_S_P5_B	25.82	2.17	0.57	0.45	0.78	16.41	1.41	0.43	0.45	26.36	4.10	0.70
RR_S_P6_A	45.48	2.75	0.35	0.46	0.68	18.84	1.35	0.50	0.48	31.02	3.64	0.81
RR_S_P6_B	96.40	3.97	0.62	0.52	0.40	18.91	0.98	0.48	0.51	36.14	3.26	1.11
RR_S_P7_	40.46	2.53	0.45	0.37	0.61	9.09	1.61	0.42	0.42	7.79	5.34	0.60

	La	Ce	Pr	Nd	Sm	Eu	Gd	Tb	Dy	Ho	Er	Tm	Yb	Lu
	DF (Al)	DF (Al)	DF (Al)	DF (Al)	DF (Al)	DF (Al)	DF (Al)	DF (Al)	DF (Al)	DF (Al)	DF (Al)	DF (Al)	DF (Al)	DF (Al)
RR_S_P4_	6.67	2.71	4.13	4.54	3.05	1.41	1.99	1.56	1.63	1.39	1.53	1.28	1.62	1.44
RR_S_P5_A	9.77	2.49	6.21	6.94	4.92	2.34	3.33	2.62	2.71	2.32	2.54	2.08	2.64	2.43
RR_S_P5_B	10.41	2.42	6.47	7.23	4.98	2.37	3.41	2.66	2.76	2.36	2.60	2.11	2.69	2.43
RR_S_P6_A	25.36	3.55	11.62	12.22	7.78	3.75	5.69	4.56	4.84	4.30	4.82	3.80	4.84	4.38
RR_S_P6_B	38.62	3.21	17.84	18.57	11.03	5.04	7.28	5.53	5.76	5.01	5.54	4.29	5.44	4.90
RR_S_P7_	5.30	2.73	3.58	4.08	3.10	1.53	2.28	1.83	2.04	1.83	2.13	1.80	2.42	2.27

5.6 Low Rare Earth Elements / High Rare Earth elements ratio (LREE/HREE)

For the evaluation of fractionation dynamics, ratios of LREE/HREE were calculated.

Table 10 shows the normalized values of rare earth elements with NASC in Rano Raraku

Table 10: Normalized values of rare earth elements with NASC in Rano Raraku

Sample	Matrix	LREE_N	HREE_N	LREE/HREE
A	Soil	3.98	9.53	0.42
B-1	Soil	2.76	6.01	0.46
B-2	Soil	2.61	5.86	0.44
C-1	Soil	1.40	3.25	0.43
C-2	Soil	0.96	3.00	0.32
D	Soil	3.55	5.01	0.71
P1-0	Filtrated	11.78	15.98	0.74
P2-0	Filtrated	8.07	14.71	0.55
P3-0	Filtrated	8.44	15.61	0.54
P1-90	Filtrated	25.90	35.30	0.73
P2-51	Filtrated	39.91	49.26	0.81
P3-38	Filtrated	15.05	23.39	0.64
P1-0	Water	1.44	9.29	0.16
P2-0	Water	1.24	8.11	0.15
P3-0	Water	0.89	7.34	0.12
P1-90	Water	3.04	10.82	0.28
P2-51	Water	0.93	7.66	0.12
P3-38	Water	1.02	8.13	0.13
P1-0	Filt + Water	13.22	25.27	0.52
P2-0	Filt + Water	9.30	22.82	0.41
P3-0	Filt + Water	9.33	22.95	0.41
P1-90	Filt + Water	28.93	46.11	0.63
P2-51	Filt + Water	40.83	56.92	0.72
P3-38	Filt + Water	16.08	31.52	0.51

As the values appears grouped depending on the matrix where they were measured, the similarity of these values was evaluated using a statistical approach, assuming that the values for each matrix belong to the same distribution that was assumed to be normal. Thus we individuated four main distributions that are: soil, water, filter and filter + water. Under this hypothesis, the Dixon test (see methodology 4.5.1) was used to individuate possible outliers.

Table 11 summarizes the results of this test.

Table 11: Presence of possible outliers in the distribution in the matrices of LREE/HREE in soil, water, filtrate and Σ (Filt+Water)

	Filtrated	Soil	Water	Σ (Filt+Water)
	0.74	0.42	0.16	0.52
	0.55	0.46	0.15	0.41
	0.54	0.44	0.12	0.41
	0.73	0.43	0.28	0.63
	0.81	0.32	0.12	0.72
	0.64	0.71	0.13	0.51
Suspect value	0.81	0.32	0.12	0.41
Q_n	0.271	0.254	0.005	0.000
Q_{critic}(95%; n=6)	0.625	0.625	0.625	0.625
Outlier	NO	NO	NO	NO
Suspect value	0.54	0.71	0.28	0.72
Q_n	0.029	0.641	0.785	0.289
Q_{critic}	0.625	0.625	0.625	0.625
Outlier	NO	YES	YES	NO

In the Table 11 it was observed that only 0.71 and 0.28 corresponding to soil and water respectively should be considered as outlier and therefore rejected. Thus, the final values considered are reported in Table 12 along with variance, Std. dev. (S) and degree freedom of groups.

Table 12: Final values of variance, Std. dev. (S) and degree freedom of groups for Rano Raraku

	Filtrated	Soil	Water	Σ (Filt+Water)
	0.74	0.42	0.16	0.52
	0.55	0.46	0.15	0.41
	0.54	0.44	0.12	0.41
	0.73	0.43	0.12	0.63
	0.81	0.32	0.13	0.72
	0.64			0.51
Mean	0.69	0.41	0.14	0.53
Variance	0.0121	0.0030	0.0003	0.015
Std. Dev. (S)	0.110	0.054	0.018	0.123
Degree Freedom	5	4	4	5

In order to check if the four groups are normally distributed, the Shapiro-Wilk test was used (see Methodology section 4.5.1). Table 13 shows the W and the p-values obtained for the four groups. Although the p-value in soil is lower than the other groups, LREE/HREE values

can still be considered as normally distributed at a confidence level of the 95%, as p-value is higher than 0.05.

Table 13: Shapiro-Wilk test of four groups

	W	p-value
Filtrated	0.91516	0.4712
Soil	0.80368	0.0868
Water	0.86684	0.2538
Σ (Filt+Water)	0.91093	0.4425

The assessment of the similarity of the variances in the four groups was performed by using the F-test (see methodology). Table 14 shows results of F-test as a ratio between the variances of four groups.

Table 14 shows detail of comparison between four groups and their F calc, F crit, p-value and the resulting homogeneity or dishomogeneity of the variance. It shows that the variances of soil vs. water and filtrated vs. water are not homogenous as Fcalc is higher than Fcrit. However, soil vs. filtrated and soil vs.Σ (Filt+Water) variances are homogeneous.

Table 14: Comparison between four groups and their Fcalc, Fcrit, p-value and Homogeneity

			Fcalc	Fcrit	p-value	Homogeneity
Soil	vs.	Filtrated	4.04	6.25	0.2004	YES
Soil	vs.	Water	9.03	6.38	0.0557	NO
Soil	vs.	Σ (Filt+Water)	5.06	6.25	0.1416	YES
Filtrated	vs.	Water	36.53	6.25	0.0039	NO

This test indicates that we can apply the t-test, but we must use the Welch-Satterthwaite for the calculation of the degree of freedom for the comparison between Soil-Water and Filtrated-Water. It must be noted that this test does not assess if the mean values are significantly similar or not. The t-test is used to assess if two means are significantly similar (see methodology). Here we are interested in the following 4 comparisons:

Table 15: Comparison of four groups values

			t calc	tcrit	p-value	Similar
Soil	vs.	Filtrated	4.98	2.32	0.001266	NO
Soil	vs.	Water	10.80	2.59	0.000137	NO
Soil	vs.	Σ (Filt+Water)	2.14	2.35	0.06872	YES
Filtrated	vs.	Water	7.82	2.53	0.00043	NO

As is evident from the Table 15, only soil values and Σ (Filt+Water) resulted significantly similar, while all the other groups were different.

5.7 Cerium Anomaly

Cerium anomaly of soil and water samples of Rano Raraku was calculated using the NASC [reference](see methodology 4.5.1) Table 16 shows the values obtained of cerium anomaly in water, soil, filtered and filter+water samples. As it is evident from Table 11a in soil sample value of cerium anomaly ranges from 1.68 to 8.44 conversely in water and filtrated sample value is not very significant.

Table 16: Values obtained for cerium anomaly in water, soil, filtered and water + soil samples

		Shale			
		Ce conc	La conc	Nd conc	
		66.7	31.1	27.4	
Sample	Matrix	Ce conc	La conc	Nd conc	Ce*(anomaly)
A	Soil	39.23	7.85	10.04	2.03
B-1	Soil	44.53	5.57	6.84	3.29
B-2	Soil	45.26	5.18	6.49	3.57
C-1	Soil	31.11	2.14	3.87	5.02
C-2	Soil	35.93	1.47	2.66	8.44
D	Soil	29.85	7.56	8.56	1.68
P1-0	Filtrated	60.28	27.56	26.57	0.99
P2-0	Filtrated	40.25	18.90	18.17	0.96
P3-0	Filtrated	39.96	18.88	19.25	0.94
P1-90	Filtrated	126.27	57.13	60.68	0.96
P2-51	Filtrated	214.70	91.29	92.62	1.04
P3-38	Filtrated	70.87	33.22	35.27	0.93
P1-0	Water	4.13	2.99	4.03	0.55
P2-0	Water	4.72	2.90	3.30	0.69
P3-0	Water	2.48	1.74	2.57	0.54
P1-90	Water	5.87	7.46	7.89	0.34
P2-51	Water	2.86	1.99	2.57	0.58
P3-38	Water	2.97	2.10	2.84	0.56
P1-0	Filt + Water	64.41	30.56	30.60	0.94
P2-0	Filt + Water	44.97	21.79	21.47	0.93
P3-0	Filt + Water	45.83	26.34	27.14	0.77
P1-90	Filt + Water	129.13	59.12	63.25	0.95
P2-51	Filt + Water	217.68	93.39	95.46	1.03
P3-38	Filt + Water	73.35	34.96	37.84	0.91

Similarity of values obtained in Table 16 was evaluated using a statistical approach; as it is evident values appeared in groups depend on the matrix where they are calculated. Thus, cerium anomaly was evaluated for main four distributed groups that are: soil, water, filter and filter + water. After that the Dixon test was used to identify possible outliers. Table 17 summarizes the results of this test. It is evident from the Table 11b in soil sample 8.44 value is outlier hence, it was rejected.

Table 17: Results obtained in Dixon test and presence of possible outliers in the distribution matrices

test-Q (Dixon)				
	Filter	Soil	Water	$\Sigma(\text{filt+water})$
	0.99	2.03	0.55	0.94
	0.96	3.29	0.69	0.93
	0.94	3.57	0.34	0.77
	0.96	5.02	0.58	0.95
	1.04	8.44	0.56	1.03
	0.93	1.68	0.54	0.91
max	1.04	8.44	0.69	1.03
min	0.93	1.68	0.34	0.77
R:	0.11	6.76	0.35	0.26
Qn(min)	0.289	0.051	0.000	0.000
Qn(max)	0.489	0.761	0.093	0.308
Qtab (95%)	0.625	0.625	0.625	0.625
Qtab (99%)	0.740	0.740	0.740	0.740

Table 18 shows the values of variance and mean in four groups (water, soil, filtered and water + soil samples). In result it is evident soil sample has large variance that is 1.77.

Table 18: values of variance and mean in four groups water , soil, filtered and water + soil samples

	Filter	Soil	Water	$\Sigma(\text{filt+water})$
	0.99	2.03	0.55	0.94
	0.96	3.29	0.69	0.93
	0.94	3.57	0.34	0.77
	0.96	5.02	0.58	0.95
	1.04	1.68	0.56	1.03
	0.93		0.54	0.91
Variance	0.00	1.77	0.01	0.01
Mean	0.97	3.12	0.54	0.92

For the evaluation of normal distribution of four groups, the Shapiro-Wilk test was used. Table 19 shows the Wand p- value calculated for the four groups. It is evident from the table that all four groups values are insignificant.

Table 19: Shapiro-Wilk test for four groups

	Filter	Soil	Water	□ (filt+water)
W	0.90	0.94	0.87	0.90
p-value	0.37	0.70	0.24	0.37

6. Discussion

As it is shown in Table 4, very high concentrations of chlorine and sodium in water samples of RR were observed. However, differently from the water, soil samples showed fewer amounts of chlorine and sodium. This could be described as Easter Island is a small island where the main source of water in the lake is rainfalls that come from South Pacific Anticyclone, the South Pacific Convergence Zone, the Intertropical Convergence Zone and the Westerly storm tracks((Margalef et al. 2013; Sáez et al. 2009). So, these precipitations bring large amount of salt with them and added into the water lake.

Moreover, Table 7 provides information that rate of evaporation is very high in RR, likely due to the high speed of winds and subtropical weather conditions. This high rate of evaporation leaves behind salt in water thus, increases salinity of the lake water.

However, in the RA the amount of sodium and chlorine found is comparative to RR is very less. This could be explain as it is evident from Table 7 rate of evaporation is very low in RA and is also fed by ground water along with rainfall (O. Margalef at al. 2014) hence they contribute to maintenance of water inorganic composition (like sodium and chlorine).

The characteristic of RR is found to be enriched in iron, silver and zinc as it is given in Table 8. Yet, it has been found that this soil is depleted in many elements as shown in Table 9 such as: sodium, cesium, lead, calcium, vanadium, nickel, strontium, potassium and rare earth elements. On visit Eater Island it was seen on Island they do not have any industry except limited agricultural practices, moreover, the island is isolated from other islands and it is not densely populated. Hence, due to these factors the island pollution is very small; it does not have pin point discharge of industries. Due to absence of these deteriorating pollution factors soil of RR is depleted in inorganic pollutants.

Increase in shrubs growth like the totora reed and tavai causes use of more elements from soil like calcium, potassium as these elements constitute structure of plants hence, they also become cause of depletion of these elements in soil.

Positive values obtained of cerium anomaly in Table 16 shows that cerium is added in nodules of RR. High values of cerium anomalies observed in soil of RR than water of lake indicates that soil is greater influenced by seawater. As larger the cerium anomaly is the smaller Mn/Fe ratios is and vice-versa. This is interpreted as soil has smallest Mn/Fe ratios thus, have small diagenetic influence and large value of cerium anomaly shows more seawater influence on nodules. Lake water has large Mn/Fe ratios and small values for cerium anomaly provide information that it is diagenetic influence (Elderfield, H, & Greaves, M. J. 1981).

As evident from the t-test, the mean values of the LREE/HREE in soil and in the system particulate-water does not significantly (95%) differ. This means that the source of RRE in the water body is due to the soil around the lake, as expected. Nevertheless, there is not a significant fractionation during the transport from the soil to the water body. The main fractionation effect takes place in the water body itself, where the particulate matter is enriched in LREE while the water is depleted.

This effect seems to contrast previous findings where the presence of chlorides should increase the solubility of LREE with respect to HREE. In this environment, as the concentration of chloride is high (about 1g/l) a different behavior should be expected. However, in the past massive deforestation and over exploitation of natural resources causes soil erosion (Azizi, G., & Flenley, J. R. 2008). When strong winds blow at an average rate of 24 km/h this favors the soil erosion process. The high speed of winds collects solid particles from the surroundings and adds into the water of the RR. Hence, this is the main factor that influenced transport dynamics inside the basin.

Table 6 shows that the RR has comparatively high amount of ammonium in their water sample and this can be explained as Figure 9b shows dead horse nearby the lake; when these horses got decayed they add waste organic and inorganic material into the lake water and release pollutants like ammonium and bromide. On visit to Island it was also observed animals directly drink water from lake moreover, they also discharge their waste in the lake. In contrast, RA no significant amount of ions like ammonium and bromide was found this is probably due to its location as it is located near to highest summit of the Island nearby population is very less and wondering animals come occasionally.

RA is drying out. This could be due to change in environmental conditions, as compare to the past Easter Island receives less amount of rainfall (Cedric O. Puleston et al, 2017). Hence, due to its location near to the top, it can easily subject to seasonal variations and even desiccation. Moreover, in 1960s plantation of eucalyptus forests near RA (V. Rull et al. 2010) and construction of artificial outlet causes significant drop of water level in the lake. As it is reported an average a eucalyptus tree uptake 11489 mm of water (Marshall, J. K et al. 1997). These are contributed factors in drying of the RA.

CONCLUSION

In this thesis I analyzed a set of water and soil samples collected in two main Lake of Easter Island. These lakes are named Rano Raraku and Rano Aroi and they currently correspond to two important source of water for agricultural practices in the island. The trace elements, isotopic and major ions analysis demonstrated that the quality of the water is not particularly polluted by heavy metals in both lakes. Nevertheless, the content of chloride and sodium resulted very high in Rano Raraku ($\sim 1 \text{ g/l-l}$) which makes the water undrinkable and not suitable for agricultural purposes. The high salt concentration is probably due to a combination of factors: firstly, the lake is quite close to the ocean and a marine input is responsible for the provision of salt (mainly NaCl). Secondly the lake is a close water body without any inflow and outflow. Thus the amount of water is controlled by evaporation/precipitation balance. Evaporation is the main contribution in recent times as it is demonstrated by the high presence of heavy oxygen isotopes in the water composition. The analysis of rare earth elements showed that there is a fractionation of the rare earth elements composition that takes place in the water body. Soil from the basin is likely transported by the winds rather than runoff as it is supported by several REE ratios. This occurrence is in agreement with the high evaporation rate hypothesized from the isotopic composition of the water. It must be noted that about 1 year after the sampling the Rano Raraku almost completely dried. From an archaeological point of view, a similar exsiccation process may had been responsible of the first Rapa Nui collapse, as hypothesized by many archaeologist about 5 centuries ago.

References

- Azizi, G., & Flenley, J. R. (2008). The last glacial maximum climatic conditions on Easter Island. *Quaternary International*, 184(1), 166-176.
- Bahn, P. G., & Flenley, J. (1992). *Easter Island, earth island* (p. 240). London: Thames and Hudson.
- Bahn, P. G., & Flenley, J. R. (2003). *The Enigmas of Easter Island*. Oxford, UK: Oxford University Press.
- Baker, P. E., Buckley, F., & Holland, J. G. (1974). Petrology and geochemistry of Easter Island. *Contributions to Mineralogy and Petrology*, 44(2), 85-100.
- Brander, J. A., & Taylor, M. S. (1998). The simple economics of Easter Island: A Ricardo-Malthus model of renewable resource use. *American economic review*, 119-138.
- Butler, K. R., & Flenley, J. R. (2010). The Rano Kau 2 pollen diagram: palaeoecology revealed. *Rapa Nui J*, 24(1), 5-10.
- Campos, L., & Peña, L. E. (1973). Los insectos de Isla de Pascua. *Revista Chilena de Entomología*, 7, 217-229.
- Cañellas-Boltà, N., Rull, V., Sáez, A., Margalef, O., Bao, R., Pla-Rabes, S., ...& Giralt, S. (2013). Vegetation changes and human settlement of Easter Island during the last millennia: a multiproxy study of the Lake Raraku sediments. *Quaternary Science Reviews*, 72, 36-48.
- Cañellas-Boltà, N., Rull, V., Sáez, A., Margalef, O., Giralt, S., Pueyo, J. J., ...& Pla-Rabes, S. (2012). Macrofossils in Raraku Lake (Easter Island) integrated with sedimentary and geochemical records: towards a palaeoecological synthesis for the last 34,000 years. *Quaternary Science Reviews*, 34, 113-126.
- Conaf-Conama-Birf, P. (1997). *Catastro y evaluación de los recursos vegetacionales nativos de Chile*. Chilean Forest Service, Santiago, Chile.
- Dalton, T. R., & Coats, R. M. (2000). Could institutional reform have saved Easter Island?. *Journal of Evolutionary Economics*, 10(5), 489-505.
- Diamond, J. (2005). *Collapse: How societies choose to fail or succeed*. Penguin.
- Dransfield, J., Flenley, J. R., King, S. M., Harkness, D. D., & Rapu, S. (1984). A recently extinct palm from Easter Island. *Nature*, 312(5996), 750.
- Dumont, H. J., Cocquyt, C., Fontugne, M., Arnold, M., Reyss, J. L., Bloemendal, J., & Zeeb, B. A. (1998). The end of moai quarrying and its effect on Lake Rano Raraku, Easter Island. *Journal of Paleolimnology*, 20(4), 409-422.
- Elderfield, H., Hawkesworth, C. J., Greaves, M. J., & Calvert, S. E. (1981). Rare earth element geochemistry of oceanic ferromanganese nodules and associated sediments. *Geochimica et Cosmochimica Acta*, 45(4), 513-528.
- Gleyzes, C., Tellier, S., & Astruc, M. (2002). Fractionation studies of trace elements in contaminated soils and sediments: a review of sequential extraction procedures. *TrAC Trends in Analytical Chemistry*, 21(6-7), 451-467.
- Grandjean, P., Bellinger, D., Bergman, Å., Cordier, S., Davey-Smith, G., Eskenazi, B., & Heindel, J. J. (2008). The faroes statement: human health effects of developmental

- exposure to chemicals in our environment. *Basic & clinical pharmacology & toxicology*, 102(2), 73-75
- Herrera, C., & Custodio, E. (2008). Conceptual hydrogeological model of volcanic Easter Island (Chile) after chemical and isotopic surveys. *Hydrogeology Journal*, 16(7), 1329-1348.
- Hunt, T. L., & Lipo, C. P. (2006). Late colonization of Easter island. *Science*, 311(5767), 1603-1606.
- Johannesson, K. H., Zhou, X., Guo, C., Stetzenbach, K. J., & Hodge, V. F. (2000). Origin of rare earth element signatures in groundwaters of circumneutral pH from southern Nevada and eastern California, USA. *Chemical Geology*, 164(3-4), 239-257.
- Kjeldsen, P., Barlaz, M. A., Rooker, A. P., Baun, A., Ledin, A., & Christensen, T. H. (2002). Present and long-term composition of MSW landfill leachate: a review. *Critical reviews in environmental science and technology*, 32(4), 297-336.
- Le, H. P., Seeman, M., Sanders, S. R., Sathe, V., Naffziger, S., & Alon, E. (2010, February). A 32nm fully integrated reconfigurable switched-capacitor DC-DC converter delivering 0.55 W/mm² at 81% efficiency. In *Solid-State Circuits Conference Digest of Technical Papers (ISSCC), 2010 IEEE International* (pp. 210-211). IEEE.
- Malik, R. N., & Nadeem, M. (2011). Spatial and temporal characterization of trace elements and nutrients in the Rawal Lake Reservoir, Pakistan using multivariate analysis techniques. *Environmental geochemistry and health*, 33(6), 525-541.
- Mann, D. H., & Meltzer, D. J. (2007). Millennial-scale dynamics of valley fills over the past 12,000 14C yr in northeastern New Mexico, USA. *Geological Society of America Bulletin*, 119(11-12), 1433-1448.
- Nunn, P. D. (2000). Environmental catastrophe in the Pacific Islands around AD 1300. *Geoarchaeology*, 15(7), 715-740.
- Orliac, C. (2000). *Fare et habitat à Tahiti* (Vol. 7). Editions Parenthèses.
- Orliac, C. (2005). The Rongorongo tablets from Easter Island: Botanical identification and 14c dating. *Archaeology in Oceania*, 40(3), 115-119.
- Puleston, C. O., Ladefoged, T. N., Haoa, S., Chadwick, O. A., Vitousek, P. M., & Stevenson, C. M. (2017). Rain, sun, soil, and sweat: a consideration of population limits on Rapa Nui (Easter Island) before European Contact. *Frontiers in Ecology and Evolution*, 5, 69.
- Qadir, A., Malik, R. N., & Husain, S. Z. (2008). Spatio-temporal variations in water quality of Nullah Aik-tributary of the river Chenab, Pakistan. *Environmental Monitoring and Assessment*, 140(1-3), 43-59.
- Rainbird, P. (2002). A message for our future? The Rapa Nui (Easter Island) ecodisaster and Pacific island environments. *World Archaeology*, 33(3), 436-451.
- Reuveny, R., & Decker, C. S. (2000). Easter Island: historical anecdote or warning for the future?. *Ecological Economics*, 35(2), 271-287.
- Rios-Rull, J. V., & Santaaulalia-Llopis, R. (2010). Redistributive shocks and productivity shocks. *Journal of Monetary Economics*, 57(8), 931-948.
- Rull, V., Cañellas-Boltà, N., Margalef, O., Pla-Rabes, S., Sáez, A., & Giralt, S. (2016). Three millennia of climatic, ecological, and cultural change on Easter Island: an integrative overview. *Frontiers in Ecology and Evolution*, 4, 29.

- Rull, V., Cañellas-Bolta, N., Margalef, O., Sáez, A., Pla-Rabes, S., & Giralt, S. (2015). Late Holocene vegetation dynamics and deforestation in Rano Aroi: implications for Easter Island's ecological and cultural history. *Quaternary Science Reviews*, 126, 219-226.
- Rull, V., Cañellas-Boltà, N., Sáez, A., Margalef, O., Bao, R., Pla-Rabes, S., & Giralt, S. (2013). Challenging Easter Island's collapse: the need for interdisciplinary synergies. *Frontiers in Ecology and Evolution*, 1, 3.
- Smedley, P. L. (1991). The geochemistry of rare earth elements in groundwater from the Carnmenellis area, southwest England. *Geochimica et Cosmochimica Acta*, 55(10), 2767-2779.
- Thomaz, S. M., & Cunha, E. R. D. (2010). The role of macrophytes in habitat structuring in aquatic ecosystems: methods of measurement, causes and consequences on animal assemblages' composition and biodiversity. *Acta Limnologica Brasiliensia*, 22(2), 218-236.
- Url: DW Article Report derived from (<https://www.dw.com/en/bringing-the-trees-back-to-easter-island/a-18366801>)
- UNESCO 2012 -
- Venter, J. C., Remington, K., Heidelberg, J. F., Halpern, A. L., Rusch, D., Eisen, J. A., & Fouts, D. E. (2004). Environmental genome shotgun sequencing of the Sargasso Sea. *Science*, 304(5667), 66-74.
- Whatley, R. C., Siveter, D. J., & Boomer, I. D. (1993). The Ostracoda. *Benton, MJ et al*, 343-356.
- Zizka, G. (1991). Flowering plants of Easter Island. *Palmarum hortus francofurtensis*; 3.